Response Surface Methodology for Predicting COD and Colour Decrease Real-time textile wastewater ozonation by adsorption upon activated Canna Indica biochar

Vishal Kumar U. Shah
Lovely Professional University
Pratima Gajbhiye
pratimawadhwani@gmail.com
Lovely Professional University
Anand Mohan Yadav
Meerut Institute of Engineering & Technology
Aparna Singh
WA School of mines, Curtin University
Aditee Pandya
P P Savani University
Md irfanul Haque Siddiqui
King Saud University
Choon Kit Chan
INTI International University
Saurav Dixit
Chitkara University
Anand Patel
University of North Texas

Article

Keywords: Adsorption, biochar, textile effluents, wastewater treatment, Koh, NaoH, ozone

Posted Date: February 6th, 2025

DOI: https://doi.org/10.21203/rs.3.rs-5956236/v1

Additional Declarations: No competing interests reported.

Response Surface Methodology for Predicting COD and Colour Decrease Real-time textile wastewater ozonation by adsorption upon activated Canna Indica biochar

Vishal Kumar U. Shah*[a,b], Pratima Gajbhiye[*], Anand Mohan Yadav[c], Aparna Singh[d], Aditee Pandya[e], Md irfanul Haque Siddiqui[f], Choon Kit Chan[g], Saurav Dixit[h], Anand Patel[i]

[a]Department of Chemical Engineering, School of Engineering, P P Savani University, Dhamdod, Kosamba, Gujarat India

[b *]Department of Chemical Engineering, School of Engineering, Lovely Professional University, Phagwara, Punjab, India

[c]Department of Chemical Engineering, Meerut Institute of Engineering & Technology, Meerut, Uttar Pradesh India

[d] WA School of mines, Minerals, Energy & Chemical Engineering, Curtin University, Perth, Australia

[e] Department of Microbiology, School of Sciences, P P Savani University, Kosamba, Surat, Gujarat 394125, India.

f Department of Mechanical Engineering, College of Engineering, King Saud University, Saudi Arabia (msiddiqui2.c@ksu.edu.sa)

g Department of mechanical engineering, INTI International University, Malaysia (choonkit.chan@newinti.edu.my)

h pro-vice chancellor, Chitkara University, Punjab, India.

[I]Department of Mechanical Engineering, University of North Texas, Denton, TX 76205, USA (akp1527@gmail.com)

Corresponding author : Vishalkumar U Shah (vishal.shah@ppsu.ac.in) & Pratima Gajbhiye (pratimawadhwani@gmail.com)

Abstract

Textile effluent comprises Colours, heavy metals, and other chemicals. Before discharge into waterways, Colour and COD should be reduced. This research used Canna Indica biochar adsorption and Ozonation to reduce COD and remove Colour. The effects of adsorbent dose, solution pH, contact duration, activating agent, and ozonation rate on COD reduction and Colour removal were examined. Potassium hydroxide-treated Canna Indica (KBC) reduced COD by 96.90% at 2.5 g/L, 8 pH, 17 hr, and 100 mL/min at ambient conditions, while sodium hydroxide-treated biochar (NBC) removed Colour at 2.5 g/L, pH 8.5, 17 hours, and 57.5 mL/min. This research found pseudo-second-order biochar adsorption in textile effluent. Chemical sorption was dominant for textile wastewater COD and Colour removal. Order of

significance: pH > adsorbent dose > contact duration > ozonation rate. KBC and NBC had maximal adsorption capacities of 357.14 mg/g and 333.33 mg/g, respectively. According to the RSM-BBD study, pH was crucial for COD and Colour removal via adsorption and ozonation. Ordering R2 isotherms according to significance Langmuir > Temkin > Redlich-Peterson > Freundlich = Halsey > Dubinin-Radushkevich for KBC and NBC. Response Surface Methodology predicts COD and Colour reduction. Approach utilizing real-time textile dye wastewater adsorption upon activated Canna Indica charcoal and ozonation

Keywords: Adsorption, biochar, textile effluents, wastewater treatment, Koh, NaoH, ozone

Graphical Abstract

Introduction

The dye, pigment, and textile industries make significant contributions to the global economy. However, they also generate large volumes of wastewater with complex chemical compositions and limited biodegradability, leading to significant environmental issues [1]. Even low levels of dyes in aquatic systems inhibit photosynthesis [2], restrict light penetration, and contribute to odour and taste concerns [3]. It is estimated that 10-15% of dyes used in operations such as desizing, mercerising, dyeing, and finishing are discharged into water bodies without being treated [4]. Azo dyes, which make up about 70% of the dye family, are particularly hazardous [5] because of their toxicity and longevity in the environment [6]. We use chemical, biological, electrochemical, and physicochemical procedures like coagulation-flocculation, electrocoagulation, membrane filtration, and advanced oxidation processes (AOPs) to effectively treat wastewater [7-9]. Adsorption is a popular approach for pollutant removal because of its efficacy, simplicity, and reusability [10-11]. Analytical techniques such as chromatographic, spectroscopic, and electrochemical approaches are critical for identifying azo dyes in food, assuring safety and regulatory compliance [12]. Electrocoagulation with iron electrodes has shown promise in the treatment of dye solutions, notably Acid Yellow 36, obtaining considerable colour removal under optimal circumstances [13]. Eco-friendly dyeing techniques based on cationic reactive dyes have also been investigated, resulting in lower water and energy usage while improving dye fixation and minimising environmental effects [14]. Heavy metal biosorption with restricted biomass in UF/MF membrane reactors reveals efficient metal removal and practical feasibility, offering a long-term option for wastewater treatment [15]. Similarly, microbial and plant-derived biomass have been evaluated as an environmentally benign and effective method of removing heavy metals from wastewater via

biosorption processes [16]. The reuse of used adsorbents, such as activated carbon, raw biomass, algae, and biochar, provides considerable environmental and economic advantages; nevertheless, obstacles and constraints remain in improving sustainability in adsorption-based pollution control methods [23]. In addition, a one-pot synthesis method inspired by bread leavening has been developed to create hierarchically [25] porous carbon for supercapacitors, resulting in materials with excellent porosity, high surface area, and superior electrochemical performance, providing a green, efficient production process [26]. Biomass pyrolysis has also been investigated for the generation of nitrogen-containing liquid chemicals and nitrogen-doped carbon compounds, demonstrating its promise for long-term chemical production and advanced material uses in energy and the environment [27]. In addition, biomass-derived carbon is developing as a flexible and high-performance material for energy storage systems, with promising applications in supercapacitors, batteries, and other advanced energy systems [28]. The univariate or one-factor-at-a-time (OFAAT) approach has considerable [29] disadvantages, including high costs, lengthy time requirements, large labour expenses, and limited insights into variable interactions [31]. Multivariate approaches are preferable to solve the constraints, because they give extensive information of variable exchanges, are more efficiency reduction, effective in cost, and require less effort and time [32]. A multivariate method incorporates both independent as well as dependent variable, Among the most often utilized methods is Response Surface Methodology (RSM) [45]. In order to better understand variable interactions and how they affect system responses, RSM employs statistical and mathematical methods to assess and improve the effects of different process factors on desired outcomes [48]. The summery of research article indicates that the method feasible for reducing COD and colour of using the canna Indica Biochar of industry effluent. Another process combined with this process is ozonation for more extreme reduce the COD and colour by applying ozone.

This Study Examine that the feasibility of using KOH and NaOH-treated activated Canna Indica leaf charcoal to remove COD and Colour from industrial effluent. Ozonation, then, is employed as a therapeutic method. Finding out how effectively adsorption and ozonation together to treat textile effluent would function in practice was the goal of this study. The optimal conditions were found by using Response Surface Methodology (RSM), which optimises the quantities of adsorbent, ozone, and time required for the process.

2. Materials and methods

2.1 Materials

Canna indica leaves were gathered from a canal near Kosamba, Gujarat, India, while wastewater samples were collected from a textile company in Kadodra, Surat, Gujarat, India.

Biochar was prepared in a custom-made SS-306 cylindrical chamber with a nitrogen cylinder for purging purposes. Central Drug House Pvt. Ltd., India, supplied analytical-grade KOH and NaOH. Pyrolysis was carried out in a muffle furnace with an operating temperature of 800-1100°C. The pH of the solution was changed by adding 0.1N HCl or 0.1M NaOH. To evaluate the colour and chemical oxygen demand (COD) of the samples, a UV-spectrophotometer (Model 893) and a COD digester were used.

2.2 Characterization

2.2.1 Scanning Electron Microscope analysis of bio-char

The samples treated with biochar underwent washing three times, each under different pretreatment conditions. After that, the samples were put in a 25% glutaraldehyde solution mixed with a 0.1 M buffering solution. They were kept at 4°C for 24 hours. After being evenly distributed on carbon paper, the samples were left in a desiccator to dry overnight. A high-resolution sputter coater was used to provide a gold coating to the samples. For a thorough study, the samples were examined using a scanning electron microscope (JSM-6500, JEOL) running at a 20 kV working voltage.

2.2.2 Fourier transform infrared spectroscopy analysis of bio-char:

Experimental finding says that how temperature, composition, and biochar dosage influence the chemical functional groups present in *Canna indica* leaves and stalks. Analysed the samples by using FTIR spectroscopy. The dried sample are weighted properly and checking the size of particle. In order to identify the Canna-Indica biochar, we also examined properties such as yield percentage, fixed carbon, volatile matter, moisture content, and the elemental makeup of carbon, hydrogen, and oxygen both proximally and ultimately. Biochar was characterised using Fourier Transform Infrared Spectroscopy (FTIR) on a Perkin Elmer Spectra 2 (USA). The scan range was 400-4000 cm^{-1}. The KBr pellet approach was applied, where dried biochar was mixed with spectroscopic-grade KBr in a 1:20 ratio, as depicted in Figure 1, for optimal FTIR measurement.

2.2.3 Brunauer–Emmett–Teller (BET) analysis of bio-char:

BET analysis is essential for examining the pore structure of synthesised biochar since it provides data on surface area, pore volume, and dispersion. A BET surface area analyser (QuantaSorb SI, Quantachrome Instruments, USA) was used to assess the porosity of untreated and processed biochar samples by N_2 adsorption/desorption isotherms at 77 K. For accurate measurements, the samples were desiccated at 50°C for 72 hours and subjected to vacuum degassing for one hour before analysis.

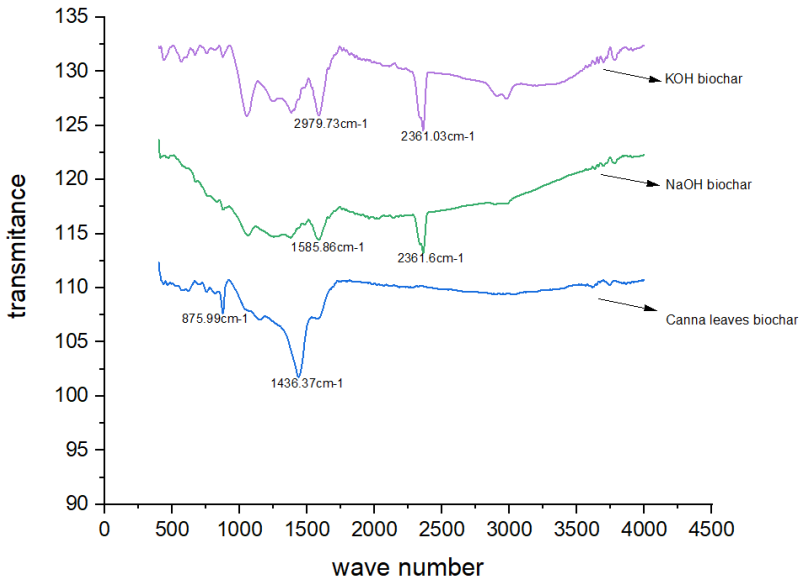

Figure 1 FTIR of Canna-Indica leaves Biochar, KOH activated biochar (KBC) and NaOH activated biochar (NBC)

A variable pressure field emission scanning electron microscope (Supra 55, Carl Zeiss, Germany) for FESEM imaging. We set it up in high vacuum mode and used a secondary electron detector. We obtained the images at magnifications ranging from 50X to 2000X, as shown in Figures 2 and 3. To find out about the adsorbent's surface area and pore size distribution, N_2 adsorption measurements at 77 K were used with Autosorb IQ-XR from Quantachrome Instruments.

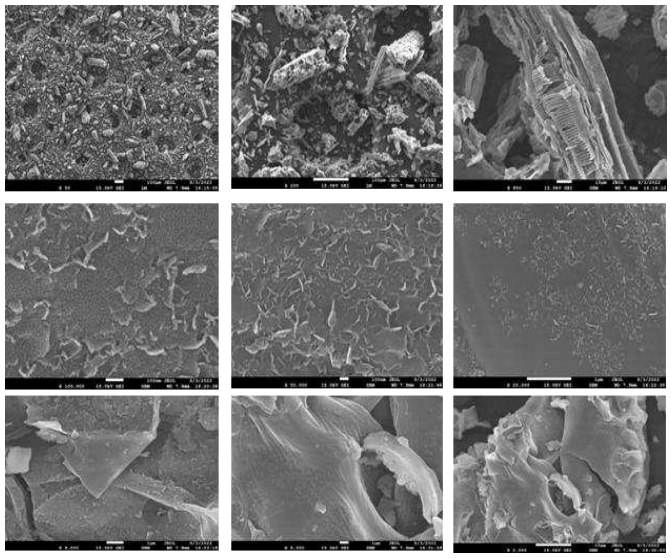

Figure 2 FESEM images of KOH Modified Biochar (KBC)

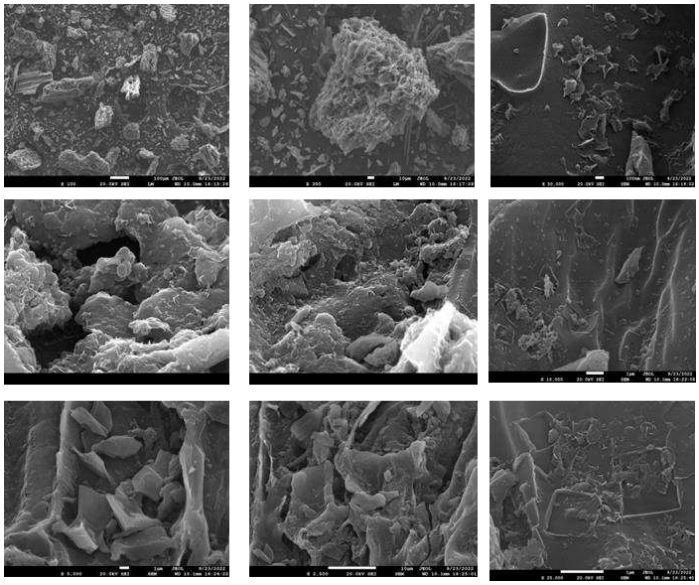

Figure 3 FESEM images of NaOH Modified Biochar (NBC)

Physicochemical characterization data in Table 1 shows 30% to 57% biochar production. The final analysis indicated KOH and NaOH affected carbon% little. The loss of oxygen-bearing functional groups in biochar caused KOH to produce more volatile stuff than NaOH. C-H stretching from aliphatic compounds is at 2979 cm^{-1}, whereas M-H stretching, which may be K-H or Na-H in KBC or NBC, is at 2361 cm^{-1}. Table 2 shows the biochar surface area increased by NaOH and KOH. KOH-activated biochar has a larger surface area, better pore distribution, and better organization than NaOH-activated and raw biochar, according to BET analysis. KOH activation releases more VM, passes K ions, and fractures and shrinks lignin and hemicellulose better than NaOH activation, increasing surface area [36]. Viewing FESEM images (Figure 2,3) demonstrates sample microstructure variations, including micropores. Different volatile chemical evolution rates may induce void production, thermal extension, and sample particle shrinkage [37]. The sawdust sample contained uniformly distributed short and coarser lignocellulosic bulk fibers. In BET studies, well-defined porous structures are caused by the release of volatile components and the breakup of polymers into smaller units in biomass Table 1.

Table 1 RSM-BBD Experimental design matrix using five variables and their respective observed results

S. No	AD	pH	CT	OR	BT	Actual % COD Removal	Predicted COD Removal	% Color Removal (Actual)	Predicted Color Removal
1	1.5	8	4	100	KBC	84.05	81.72	75.33	75.49
2	0.5	10	10.5	57.5	KBC	61.43	57.12	68.67	67.88
3	1.5	8	17	100	KBC	96.67	99.10	85.00	86.77
4	0.5	6	10.5	57.5	KBC	57.62	61.14	58.20	58.31
5	1.5	10	10.5	100	KBC	71.90	75.72	73.00	72.04
6	2.5	6	10.5	57.5	KBC	79.52	80.77	70.27	70.82
7	2.5	8	10.5	100	KBC	94.52	93.82	93.67	93.07
8	2.5	8	10.5	15	KBC	84.76	85.78	86.00	85.89
9	0.5	8	10.5	100	KBC	80.71	79.02	82.80	80.56
10	1.5	8	10.5	57.5	KBC	85.95	85.60	77.92	77.54
11	1.5	10	4	57.5	KBC	60.00	62.22	61.53	59.55
12	1.5	8	4	15	KBC	70.95	68.86	67.93	68.32
13	1.5	8	17	15	KBC	86.19	86.24	80.07	79.59
14	1.5	10	10.5	15	KBC	57.14	62.86	63.73	64.87
15	0.5	8	4	57.5	KBC	59.76	59.30	69.53	73.16
16	1.5	8	10.5	57.5	KBC	85.95	85.60	77.92	77.54
17	1.5	8	10.5	57.5	KBC	85.95	85.60	77.92	77.54
18	1.5	6	10.5	15	KBC	69.76	66.89	54.33	55.29
19	1.5	8	10.5	57.5	KBC	85.95	85.60	77.92	77.54
20	1.5	6	10.5	100	KBC	81.90	79.74	58.67	62.47
21	2.5	8	4	57.5	KBC	86.19	86.55	79.67	82.02
22	2.5	8	17	57.5	KBC	94.52	96.31	99.00	96.94
23	2.5	10	10.5	57.5	KBC	80.95	76.74	79.00	80.39
24	1.5	8	10.5	57.5	KBC	85.95	85.60	77.92	77.54
25	1.5	6	4	57.5	KBC	66.19	66.25	62.00	56.51
26	1.5	6	17	57.5	KBC	84.76	83.63	62.07	61.26
27	0.5	8	10.5	15	KBC	62.86	61.34	73.33	73.38
28	0.5	8	17	57.5	KBC	82.14	84.31	81.87	80.78
29	1.5	10	17	57.5	KBC	83.10	79.61	75.00	77.35
30	0.5	8	17	57.5	NBC	81.43	82.12	81.00	79.59
31	1.5	6	17	57.5	NBC	81.90	81.45	61.31	60.06
32	1.5	6	10.5	15	NBC	67.62	64.70	53.00	54.10
33	1.5	8	10.5	57.5	NBC	83.81	83.42	75.98	76.35
34	1.5	10	10.5	15	NBC	55.95	60.68	63.33	63.67
35	2.5	8	10.5	15	NBC	83.81	83.60	85.33	84.70
36	2.5	10	10.5	57.5	NBC	79.76	74.56	78.33	79.20
37	1.5	10	17	57.5	NBC	80.48	77.42	74.00	76.16
38	2.5	6	10.5	57.5	NBC	76.67	78.58	68.53	69.63
39	0.5	8	10.5	15	NBC	59.52	59.16	71.99	72.19

40	0.5	8	10.5	100	NBC	79.76	76.84	81.99	79.36
41	2.5	8	4	57.5	NBC	82.38	84.37	79.33	80.83
42	1.5	8	17	100	NBC	95.48	96.91	83.67	85.58
43	1.5	10	4	57.5	NBC	58.10	60.04	60.67	58.36
44	1.5	8	10.5	57.5	NBC	83.81	83.42	75.98	76.35
45	2.5	8	17	57.5	NBC	92.62	94.13	98.92	95.75
46	1.5	6	10.5	100	NBC	80.00	77.56	57.85	61.28
47	2.5	8	10.5	100	NBC	92.86	91.64	93.00	91.88
48	1.5	6	4	57.5	NBC	64.76	64.07	60.67	55.31
49	1.5	8	17	15	NBC	85.24	84.06	79.00	78.40
50	1.5	8	10.5	57.5	NBC	83.81	83.42	75.98	76.35
51	0.5	8	4	57.5	NBC	54.76	57.12	69.00	71.96
52	1.5	8	4	15	NBC	67.14	66.68	66.60	67.13
53	0.5	6	10.5	57.5	NBC	54.76	58.96	55.20	57.12
54	1.5	10	10.5	100	NBC	70.00	73.54	72.33	70.85
55	1.5	8	10.5	57.5	NBC	83.81	83.42	75.98	76.35
56	0.5	10	10.5	57.5	NBC	58.33	54.93	67.33	66.69
57	1.5	8	10.5	57.5	NBC	83.81	83.42	75.98	76.35
58	1.5	8	4	100	NBC	81.67	79.53	73.40	74.30

Table 2 % Yield Pore Volume and BET Surface area of Canna Indica char activated using KOH and NaOH

Pyrolysis Temp. (°C)	**% Yield**		**Pore Volume**		**BET Surface area (m^2/g)**		
	KBC	**NBC**	**KBC**	**NBC**	**BC**	**KBC**	**NBC**
400	57.21	55.12	0.01	--	5.81	24.98	18.23
600	54.19	51.23	0.04	0.03	16.83	56.23	48.52
800	47.94	43.24	0.11	0.09	43.70	128.91	91.29
1000	32.18	30.14	0.14	0.11	65.33	151.56	120.15

2.3 Preparation of *Canna-Indica* Biochar

Canna-Indica leaves and stems were washed three or four times with tap water before being sun-dried for 2-3 days to make biochar. The dried leaves and stems were then chopped into 1–2 cm pieces. These smaller fragments were pyrolyzed at 500 degrees Celsius. Following pyrolysis, the resultant biochar was pulverised and kept in airtight plastic bags. KBC and NBC solutions were injected with charcoal, filtered, and dried at 90°C to produce a consistent weight. The impregnated biochar was pyrolyzed under the same circumstances for two hours before

cooling, grinding, washing with a neutral solution, drying, and packaging for testing. Table 3 shows the proximate and final analyses of raw and generated biochar.

Table 3 Proximate and Ultimate Analysis of Canna Indica leaves

	Proximate Analysis (%)				**Ultimate Analysis (%)**				
	M_t	A_d	V_{daf}	FC_{daf}	C_{daf}	H_{daf}	O_{daf}	N_{daf}	S_{daf}
RS	13.56	13.00	47.19	52.81	49.00	8.58	23.34	11.13	7.94
KBC	2.13	28.77	8.94	91.06	87.05	2.21	1.09	6.83	2.82
NBC	2.45	30.05	13.44	86.56	82.28	3.87	0.94	9.29	3.62

M: moisture; A: Ash; d: dry; V: volatile; FC: Fixed carbon; daf: dry ash free basis; *

2.4 Batch Experiments for Adsorption-Ozonation

KOH/NaOH-impregnated chars were used in several investigations to establish adsorbent dose and range. Each variable was optimized for maximum Colour removal and COD reduction. Early variable range optimization trials showed uniformly spaced levels. Dilution using distilled water decreased industrial effluent concentration.

These batch experiments used mechanical stirrers. For pH control, 100 mL of wastewater was placed in a 250 mL flask at room temperature. Adsorbent (0.5-2.5 g/L) was applied at 150 rpm for 0-17 hours. After contacting for the appropriate duration (0-17 h), the adsorbent was filtered out and the filtrate was collected for further research. Analysing three samples reduced experiment errors. Ozone was applied to the filtrate solution at 15-100 mL/min for 15 minutes. The solution was examined for Colour and chemical oxygen demand after precipitates were removed. % COD and Colour removal were calculated by Equation. (1) and (2).

$$\% \text{ COD Removal} = \left(\frac{D_i - D_f}{D_f}\right) \times 100 \tag{1}$$

$$\% \text{ Color Removal} = \left(\frac{C_i - C_f}{C_f}\right) \times 100 \tag{2}$$

Where D_i, D_f are the initial and final COD concentrations respectively, and C_i and C_f are the initial and final color concentrations in the solution, respectively.

The adsorption capacity of dye color by *Canna Indica* at equilibrium was calculated by applying equation (3)

$$Q_e = \frac{(C_i - C_f) \times V}{W} \tag{3}$$

Where, C_i, C_f, V and W are initial color concentration, final color concentration, Volume of solution taken, and amount of adsorbent added to the solution, respectively.

2.5 Response Surface Methodology

This study used the Box-Behnken Design (BBD) of Response Surface Methodology (RSM) to assess the impact of process factors such as adsorbent dose [35], contact duration, pH, type of activated biochar, and ozonation rate on COD and colour removal [41]. Here some factors are modified based on the combine adsorption process with ozonation technic [45]. The things were totally new for the industrial waste water treatment for utilizing the efficiency of chemical oxygen demand and colour [57]. A comprehensive understanding of the process dynamics and the creation of ideal operating parameters for enhanced treatment efficacy were made possible by this approach [46–48].

Table 4 Experimental ranges and levels of the factor used in the BBD design

Variables	Coded Symbol	Levels and Range		
		-1	0	1
Adsorbent dosage (g/L)	AD	0.5	1.5	2.5
pH	pH	6	8	10
Contact time (h)	CT	4	10.5	17
Ozonation rate (mL/min)	OR	15	57.5	100
Biochar type	BT	NBC		KBC

The experiment's RSM-BBD design was based on three levels of four numeric factors (adsorbent dose (g/L), pH, contact duration (h), and ozonation rate (mL/min), as well as two levels of one categorical variable (kind of activated biochar), as stated in Tables 1–4. RSM-BBD Table 4 DOE defined 58 experimental runs, five of which were in the centre points of each activated biochar, as shown in Table 2. Equation (4) represents the fitted quadratic response model [34].

$$y = \beta_o + \sum_{j=1}^{k} \beta_j x_j + \sum_{j=1}^{k} \beta_{jj} {x_j}^2 + \sum\sum_{i<j}^{k} \beta_{ij} x_i x_j + \varepsilon \quad (4)$$

In this study, the predicted output values (% COD removal and % Colour removal) are represented by y, while βo denotes the constant term, βj represents the linear coefficients, βjj refers to the quadratic coefficients, βij indicates the interaction coefficients, and ε represents the error term [49-51]. All tests were carried out in triplicate, and the average findings were utilised in the Box-Behnken Design (BBD) analysis, as shown in Table 1 [52]. The BBD-DOE study was performed using Design Expert 7.0 software (STAT-EASE Inc., USA). Model quality was assessed using the ANOVA F-value, p-value, coefficient of determination, and modified coefficient of determination. [53].

3. Result and Discussion

Numerous tests with varied adsorption doses were carried out in order to assess the influence of a wide range of factors on waste water and biochar, and the results of these experiments were analyzed in order to come to a conclusion. In addition to that, the response surface

techniques are used in this study to evaluate the adsorption behavior and isotherm features of biochar. As activating agents for the biochar, both potassium hydroxide (KOH) and sodium hydroxide (NaOH) were used in a variety of experimental runs.

3.1 FE-SEM Analysis of Biochar

The porous structure of the biochar is demonstrated by the scanning electron microscopy (SEM) images in Figure 4, which also show its large surface area, which allows it to adsorb a wide range of chemicals, including organic contaminants and heavy metals. The EDX mapping results show that the biochar contains a variety of mineral components, such as carbon, oxygen, sodium, chlorine, and potassium, which are essential for lowering COD during wastewater treatment. Additionally, the mineral component of the biochar helps with carbon sequestration by enhancing the stability of organic carbon within the biochar matrix. Figures (a) and (c) exhibit magnifications of 100 µm for Canna indica leaves and 1 µm for Canna stems.

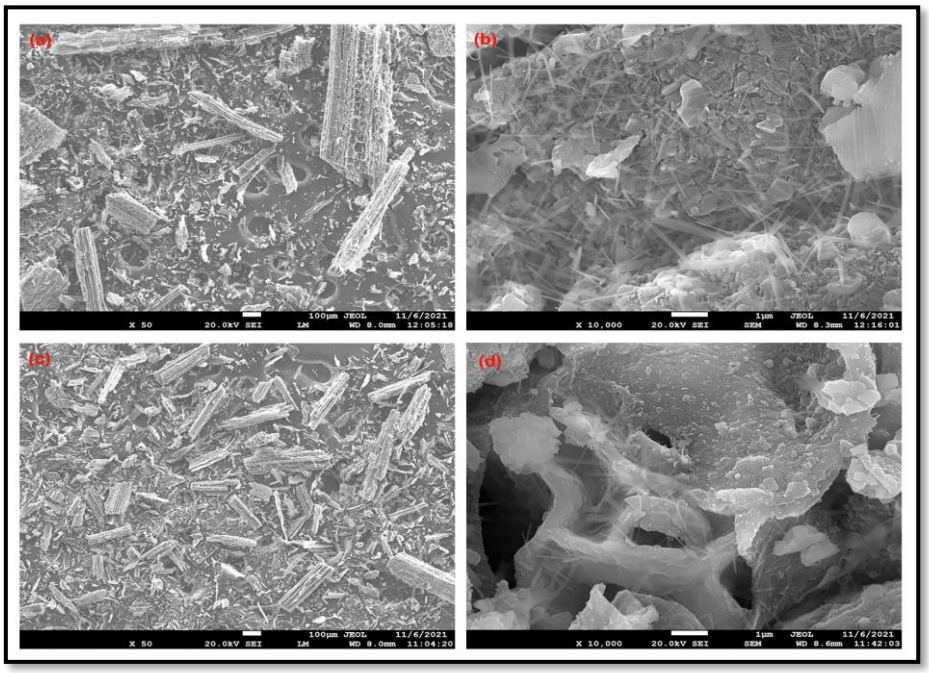

Figure 4 FESEM analysis of Canna Indica Leaves (Fig a, c) and Canna Stalk Biochar (Fig b, d)

3.2 FTIR Analysis of biochar

The FTIR analysis of biochar provides valuable insights into its functional groups, chemical bonding, and molecular structure. Figure 5 illustrates the infrared light transmittance across the range of 400 to 4000 cm^{-1}, showcasing the various functional groups present in the biochar. Biochar typically contains several functional groups, such as hydroxyl, carboxyl, carbonyl, and aromatic groups. Finding out the FTIR peaks at 800 to 1800 $cm^{-1,}$ based on the stretching and

bending of different bond like hydrogen-carbon, oxygen-carbon, and carbon-carbon. As per the method some picks are got the different design based on different feedstock and the method used for pyrolysis for production of biochar. The all pics and spectra are shown in figure 5, lower portion shows that the spectra of the canna-indica leaves biochar and the red color portion are for the canna-indica stalk biochar. The existence of carboxylic acid and oxygen and hydrogen bonds is shown by the FTIR measurement, which shows a signal at 1436 cm^{-1}. Samples of biochar frequently exhibit these characteristics. The carbon and hydrogen group are also detectable at 875 cm^{-1}.

Through laboratory investigation of Canna leaf and stalk samples, the FTIR spectra were acquired, providing additional proof of the biochar's chemical traits and functional categories. These findings advance our understanding of the adsorption properties of biochar and its possible future applications.

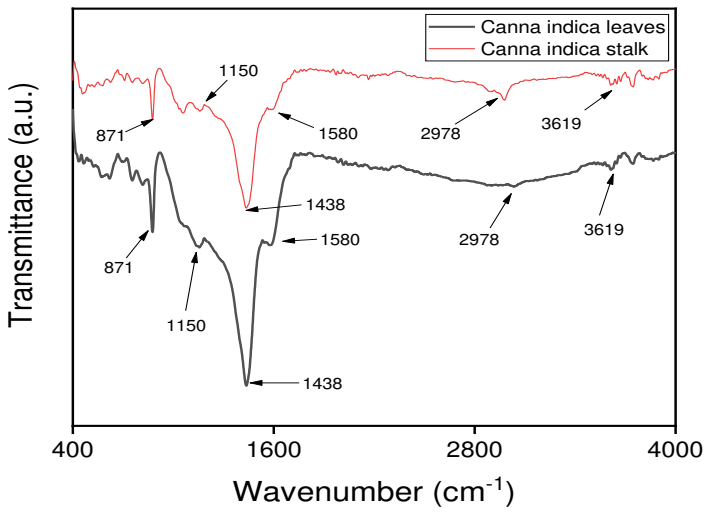

Figure 5 FTIR analysis of Canna Indica Leaves (Black Color) and Canna Indica Stalk Biochar (Red Color)

3.3 BET Analysis

One popular technique for determining the surface area of solid materials is the Brunauer-Emmett-Teller (BET) analysis. The characteristics of biochar, including its capacity to retain nutrients, adsorb chemicals, and promote microbial activity, are largely determined by its surface area. Based on the process the thickness is directly related with the volume. The method is giving the idea about the proper surface area of particular particle which are used in adsorption process. One specialised tool used in BET analysis is a degassing station. By performing adsorption isotherms, this station shows how the amount of gas adsorbed and the ambient pressure are related. For more calculating the surface area we have to go for the

additional technic to understanding of particle size. Different technology used like mercury intrusion porosimetry for more finding the porosity of the particle. In order to enable the use of biochar in a variety of applications, such as energy storage, agriculture, and environmental remediation, this work emphasises the importance of BET analysis in offering crucial insights into its properties. More in-depth understanding of the pore structure of biochar is frequently achieved by using sophisticated techniques like DFT approaches and BJH (version 3.01). The potential of biochar in a variety of fields may be thoroughly assessed thanks to these approaches, especially when it comes to improving industrial applications' efficiency and sustainability.

Table 5 BET Comparison with International slandered data

Sr. No	International Standards of pore diameter for Adsorption		Pore volume of biochar cc/g	Pore radius (°A)	Surface area (m^2/gm)	Average pore radius (nm)
1	Micropores (<2nm), Mesopore (2-50 nm) and Macropores (50nm<	Before	0.030	17.893	20.199	1.9578
2		After	0.016	15.432	11.937	3.656

The results of the BET analysis from the biochar are summarized in Table 5. The value of our biochar is clearly evident through its compliance with the global pore diameter standard. In this scenario, various metrics, including pore volume, pore radius, surface area, and average pore radius of biochar, were assessed for both the initial and final measurements. The findings distinctly indicate a notable increase in surface area, escalating from 11.937 to 20.199 m²/gm. The average pore radius decreased from 3.656 nm to 1.9578 nm.

3.4 Effect of process variables

3.4.1 Effect of pH

One of the most significant adsorption parameters is solution pH, which impacts ionization and chemical speciation. This study employed 1.5–14 pH. KOH-activated biochar (KBC) decreased COD (96.67%) and Colour (99.10%) the highest at pH 8, whereas NaOH-activated biochar (NBC) lowered 95.48%) and Colour (96.91%). K+ ions at the biochar surface travel through biomass's porous structure to distribute and shape its pores, unlike Na+ ions [38]. attribute it to ozone and hydroxyl interacting with substrate. Ozone was a major oxidizer at pH

6, but in a slightly alkaline medium (pH 8), it transformed into a hydroxyl radical and a very active radical at pH 10, although poorer selectivity at pH 10 lowered COD and Colour.

3.4.2 Effect of adsorbent dosage

This study looked at how different adsorbent doses affected COD and colour removal effectiveness, with dosages ranging from 0.5 to 2.5 g/L. Increased adsorbent dose results in a greater number of unoccupied adsorption sites while retaining a consistent quantity of adsorbate. The initial COD of the industrial effluent was measured at 2100 mg/L. At the lowest adsorbent dose of 0.5 g/L, COD removal efficiency was 57.14% with KBC and 54.76% with NBC. When the dose was raised to 2.5 g/L, COD elimination improved dramatically, reaching 96.67% with KBC and 95.48% with NBC. Similarly, colour removal at 0.5 g/L was detected at 57.12% for KBC and 54.93% for NBC, but maximum removal rates of 99.10% and 96.91% were obtained for KBC and NBC, respectively, at 2.5 g/L (as shown in Figures 6-9). The observed increase in removal effectiveness at larger doses is due to the increasing ratio of active adsorption sites to adsorbate concentration, which increases the system's adsorption capacity. Furthermore, KBC demonstrated improved efficacy because of its more effective pore dispersion, which enhanced the possibility of adsorbates being trapped in the pores [39]. BET research demonstrated that KBC has a wider pore radius than NBC, allowing for improved adsorbate accessibility and resulting in more effective removal. These findings highlight the crucial significance of adsorbent dose and material parameters in optimising COD and colour removal from industrial wastewater [40].

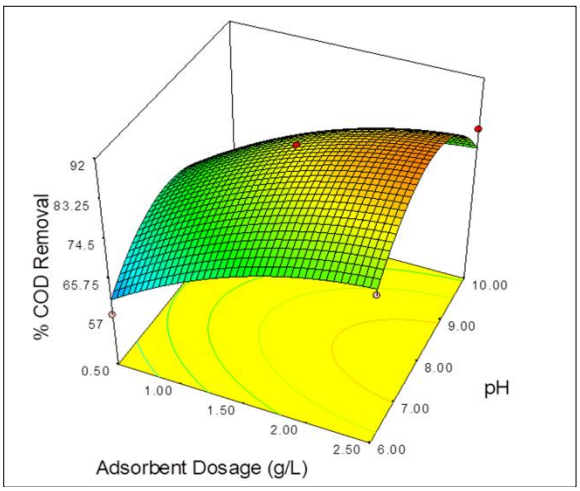

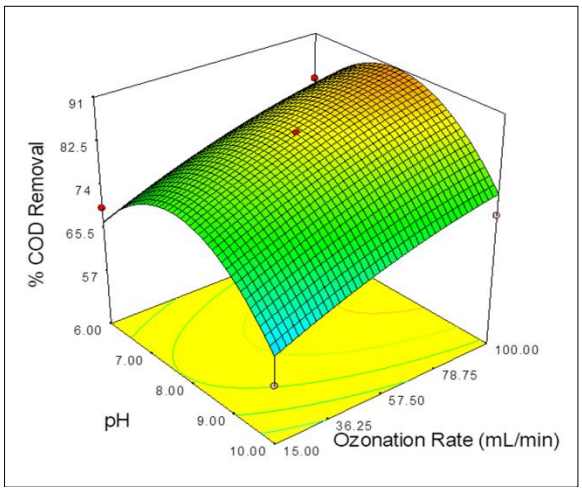

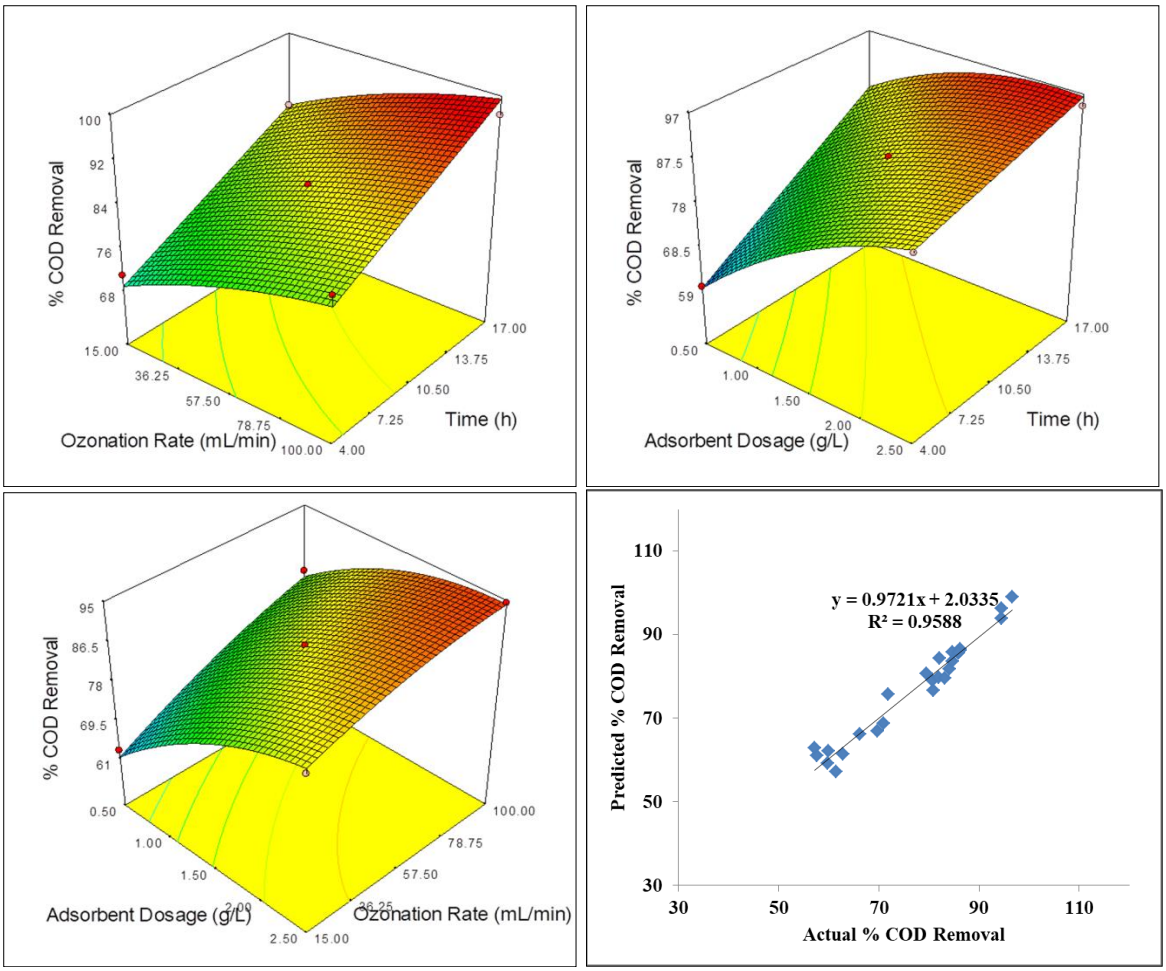

Figure 6 Effect of process variables on % COD removal using KBC

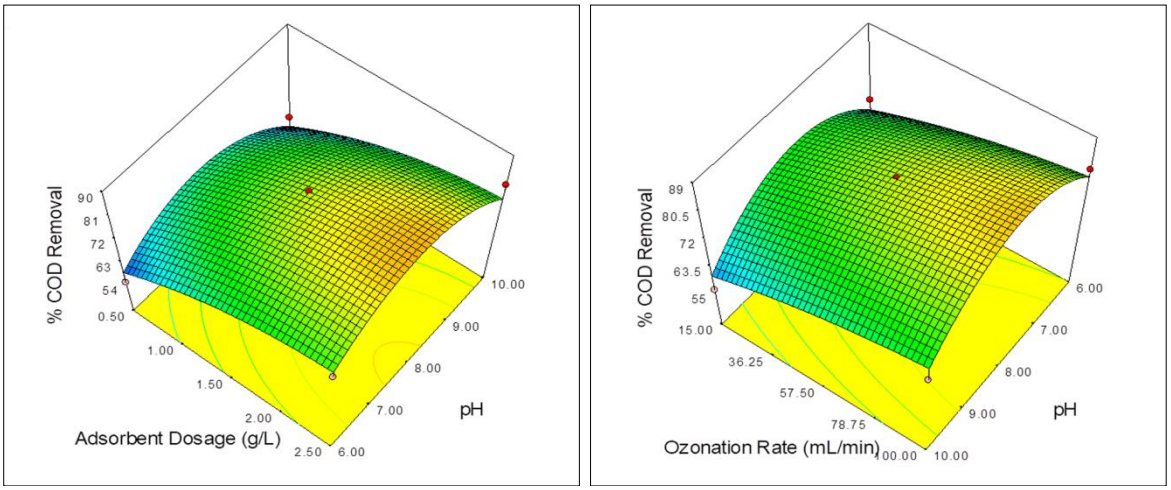

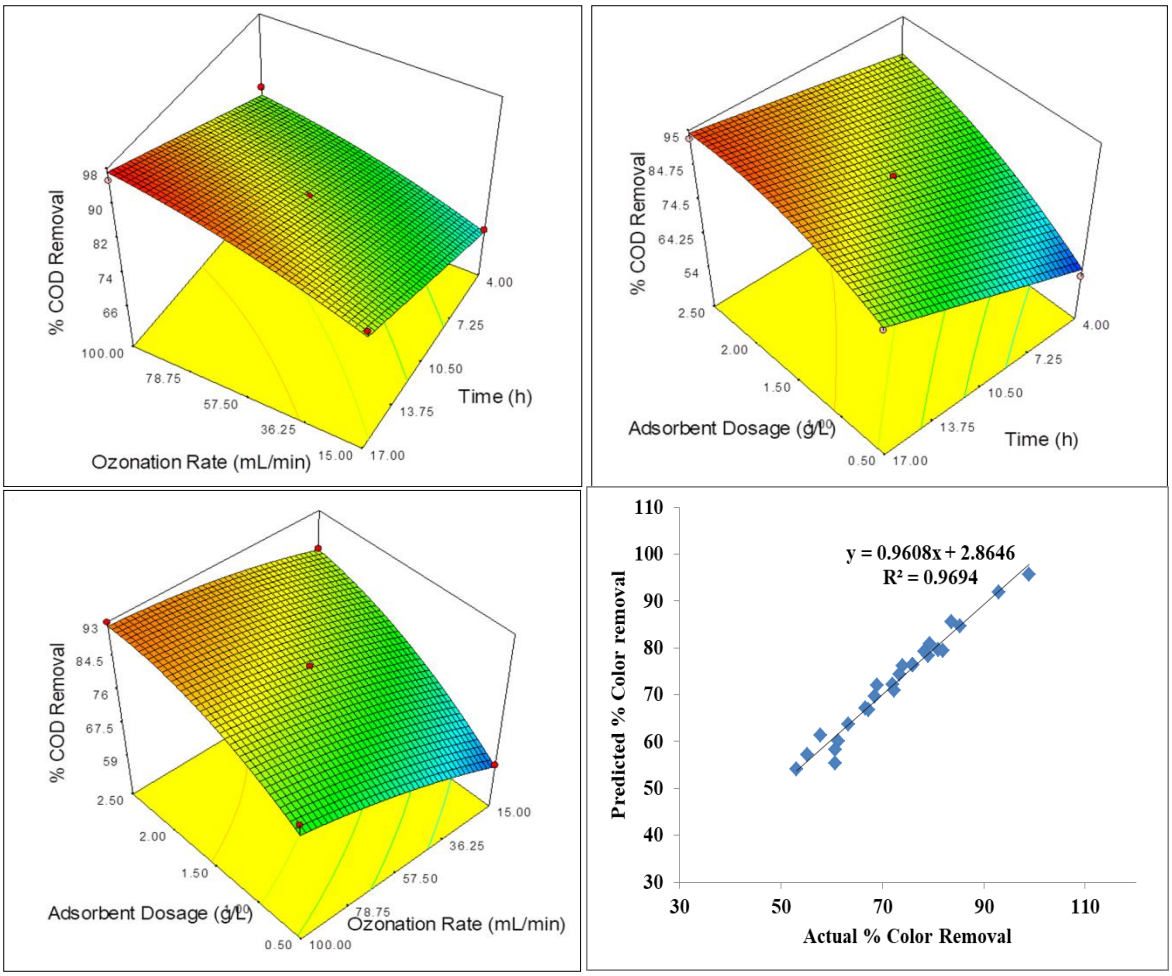

Figure 7 Effect of process variables on % COD removal using NBC

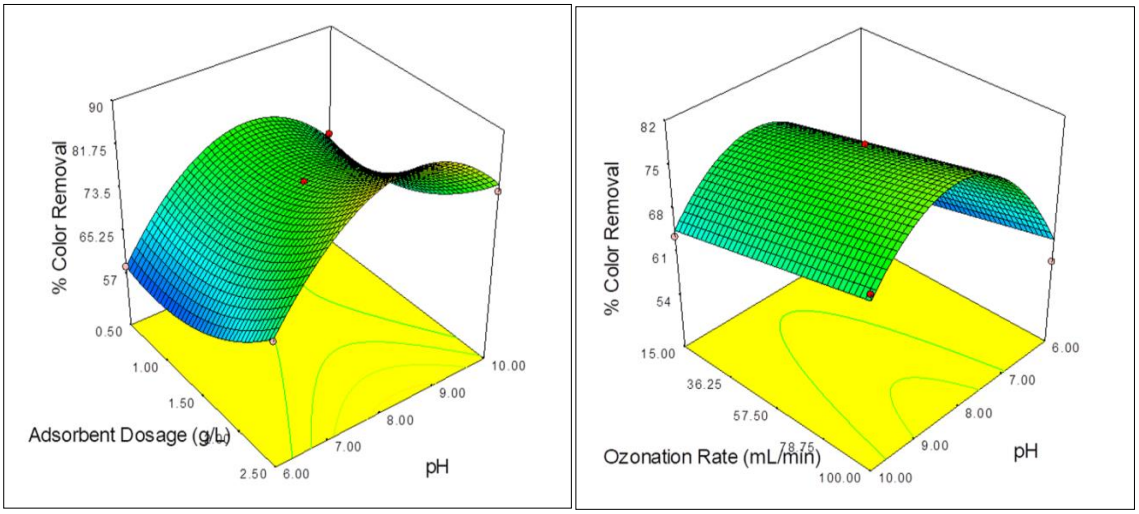

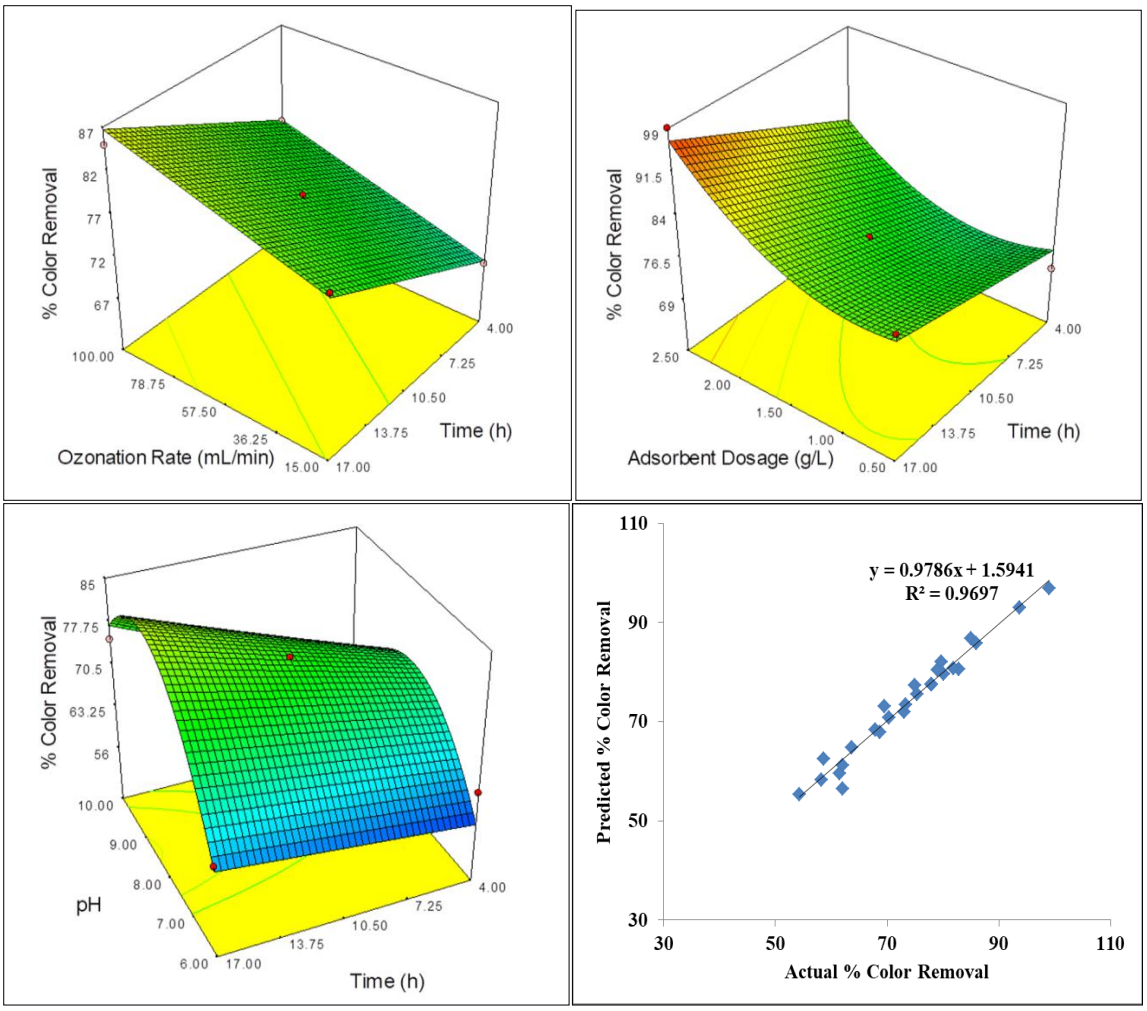

Figure 8 Effect of process variables on % Color removal using KBC

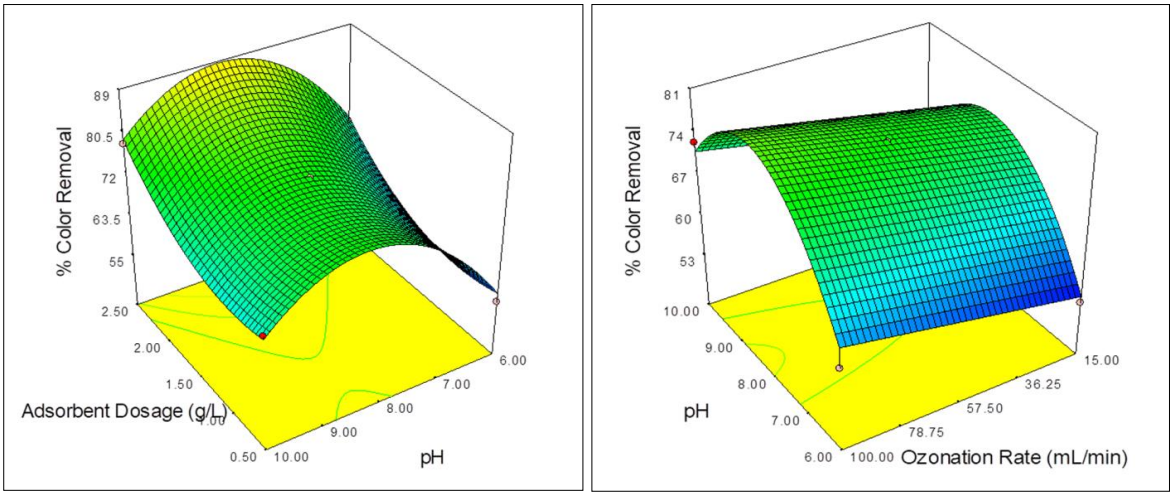

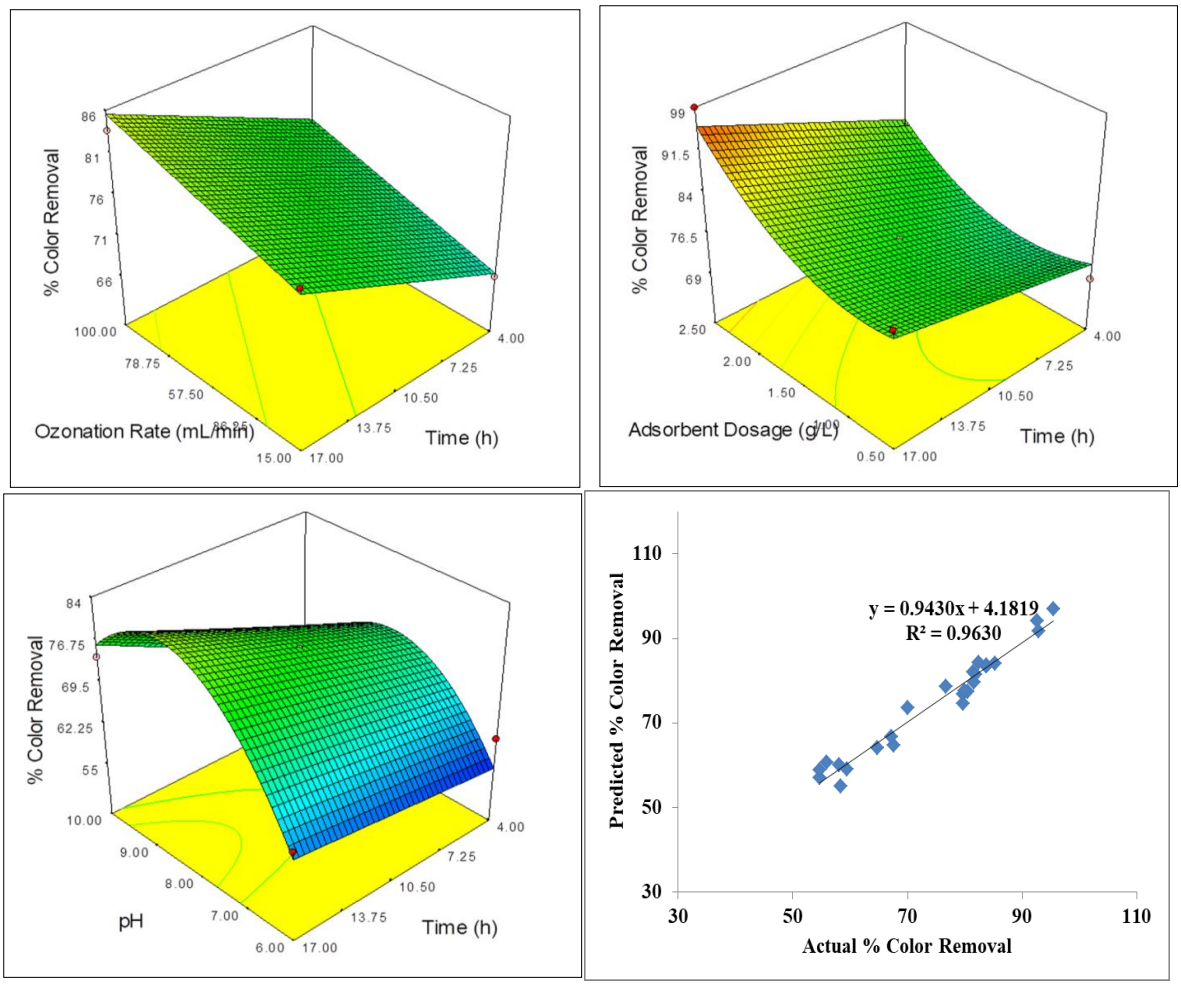

Figure 9 Effect of process variables on % Color removal using NBC

3.4.3 Effect of contact time

The contact period is critical for removing COD and colour with KBC and NBC adsorbents. As contact time extended, both Chemical Oxygen Demand and colour reduce drastically. After completing the process, the adsorbent and adsorbate are absorbed on the biochar more and more after filtration process [41]. Over time, the rate of removal slowed as adsorption sites were saturated, resulting in a less transfer of mass based on the rate. The saturation time of the content removal for fourteen hours based on the adsorbent dose from 0.5 to 2.5 grams/l, but the dropped started from 9 hours when we put the concentration 2.5 gram/l. the new observing detail with another comparable patterns in the adsorption process, from where the effectiveness of reactant to product removal is influenced by both define contact time and proper adsorbent dosage [42].

3.4.4 Effect of Ozonation

Due to its ability to break double bonds and the processes that include ozone and hydroxyl radicals, which are particularly reactive in some situations, ozonation has been shown to be an effective method for getting rid of COD and colour, and by adjusting the ozonation rate in combination with adsorption parameters, this study sought to evaluate the impact of ozonation

on COD and colour removal. Based on adsorption alone was insufficient for successfully eliminating Chemical Oxygen Demand and water colour [43]. As the time contact increases based on that the chemical oxygen demand and colour change, gives good result in reduction. The reaction based on the bond breaking and new ozone radical bond are attached, after attaching that the organic content reduces. Ozone also caused organic and inorganic pollutants to reach higher oxidation states, which allowed them to be released and further reduced COD. Investigations have shown similar outcomes [44].

The effect of ozonation was found significant with low adsorbent dosage in comparison to high adsorbent dosage, which can be attributed to the high presence of impurities present in the system at low adsorbent dosage. The ozonation may have affected the surface charges of adsorbent enabling the multilayer adsorption which in turn resulted in high adsorption capacity of adsorbent at lower dosage in comparison to higher dosage.

3.5 Adsorption Kinetic Study

Distinct kinetic models, including pseudo-first order (PFO), pseudo-second order (PSO), and intra-particle diffusion (IPD), were employed to investigate the kinetics of adsorption. The pseudo-first order (PFO) model indicates that the rate of adsorption is directly related to the availability of unoccupied sorption sites or the concentration of ions still present in the solution. The linear form is described by equation (5).

$$log(q_e - q_t) = log q_e - \left(\frac{k_1 t}{2.303}\right) \tag{5}$$

The pseudo-second-order (PSO) model includes chemisorption and the equation in linear form is as follows (equation 6)

$$\frac{t}{q_t} = \frac{1}{k_2 q_e^2} + \frac{t}{q_e} \tag{6}$$

The initial rate of intra-particle diffusion is calculated by the intra-particle diffusion (IPD) model and the equation can be expressed as (equation 7):

$$q_t = k_{diff}\ t^{0.5} + C \tag{7}$$

In this instance, qt and qe symbolizes the amount of adsorbate that has been adsorbed at time t and at equilibrium, respectively. The rate constants K_1 and K_2 correspond to the pseudo-first order (PFO) and pseudo-second order (PSO) kinetic models, respectively. K_{diff} (mg/g.min$^{0.5}$) indicates the rate constant for intra-particle diffusion, while t denotes the duration of contact (min). The intercept provides the constant C, which correlates with the thickness of the

boundary layer. A greater C value signifies a more pronounced influence of the boundary layer on the adsorption process.

Table 6 Kinetic parameters for real-time textile effluent adsorption onto KBC KOH activated biochar

Model	Initial Conc.	1000			1500			2000			2500		
	Adsorbent dosage (g/L)	0.5	1.5	2.5	0.5	1.5	2.5	0.5	1.5	2.5	0.5	1.5	2.5
PFO	q_{exp}	155.00	57.53	37.60	229.20	84.00	54.20	292.80	109.87	69.68	309.00	129.33	82.32
	k_1 (10^{-3})	4.84	4.84	4.15	5.53	5.07	5.30	5.30	5.07	5.53	5.07	5.07	5.07
	q_{cal}	222.59	70.06	44.44	267.49	84.82	66.08	355.80	128.00	86.46	361.41	144.78	88.92
	R^2	0.9226	0.9449	0.9262	0.9531	0.9522	0.9395	0.9372	0.9410	0.9321	0.9153	0.9143	0.9217
PSO	k_2 (10^{-4})	12.49	63.55	87.35	23.40	79.94	95.51	17.49	47.60	80.15	18.54	48.45	80.14
	q_{cal}	217.39	70.92	46.30	270.27	95.24	63.29	344.83	128.21	80.65	357.14	147.06	92.59
	R^2	0.9975	0.9994	0.9928	0.9992	0.9997	0.9977	0.9978	0.9974	0.9970	0.9966	0.9967	0.9967
IPD	k_{diff}	5.4277	1.8148	1.1720	6.6111	2.2766	1.5589	8.3977	3.1304	1.9461	8.3999	3.4107	2.1372
	C	3.7901	5.3384	2.6199	42.861	19.805	9.5165	52.128	19.824	13.87	65.6190	30.511	20.345
	R^2	0.9776	0.9489	0.9833	0.9151	0.8942	0.9492	0.9483	0.9517	0.9503	0.9568	0.9444	0.9443

Table 7 Kinetic parameters for real-time textile effluent adsorption onto NBC NaOH activated biochar

Model	Initial Conc.	1000			1500			2000			2500		
	Adsorbent dosage (g/L)	0.5	1.5	2.5	0.5	1.5	2.5	0.5	1.5	2.5	0.5	1.5	2.5
PFO	q_{exp}	148.00	55.87	36.80	218.40	82.00	53.20	278.80	107.20	68.40	292.40	125.67	80.40
	k_1 (10^{-3})	5.76	5.30	5.76	5.99	6.22	5.76	5.76	5.76	5.53	5.76	5.30	5.07
	q_{cal}	244.29	77.62	54.88	283.04	115.66	71.25	377.05	149.86	91.26	359.09	148.39	87.92
	R^2	0.9035	0.9286	0.9110	0.9348	0.9256	0.9351	0.9189	0.9053	0.8983	0.9348	0.9145	0.9374
PSO	k_2 (10^{-4})	14.58	55.78	93.30	23.81	57.85	89.02	16.65	43.87	76.96	20.74	49.97	80.29
	q_{cal}	204.08	70.92	46.08	256.41	98.04	63.29	333.33	126.58	79.37	333.33	142.86	90.91
	R^2	0.9965	0.9976	0.9986	0.9989	0.9986	0.9976	0.9977	0.9949	0.9962	0.9987	0.9966	0.9969
IPD	k_{diff}	5.1674	1.8211	1.1862	6.443	2.4581	1.5763	8.2052	3.1294	1.9346	8.1423	3.3301	2.1211
	C	0.87	3.26	2.87	37.57	12.52	8.22	43.47	16.74	12.55	61.32	29.58	19.25
	R^2	0.9675	0.9658	0.9540	0.9129	0.9369	0.9495	0.9518	0.9649	0.9583	0.9321	0.9461	0.9443

Figures 10-12 show the adsorption performance of the PFO, PSO, and IPD models at adsorbent doses of 0.5, 1.5, and 2.5 g/L. Figures 10-12, as well as Tables 5 and 6, show that real-time industrial effluent adsorption is more closely aligned with the PSO model, with a better correlation coefficient (>0.99) than the PFO model (>0.91) for the investigated adsorbent doses and starting concentrations. The predicted maximum adsorption capacity from the PSO model was closer to the experimental values than the PFO model, showing that the adsorption process mostly followed the PSO mechanism. These results show that the adsorption of textile effluent over KOH-activated Canna indica charcoal is predominantly controlled by chemisorption rather than physisorption.

The observed maximum adsorption capacities were 309 mg/g for KBC and 292.14 mg/g for NBC, although theoretical estimations anticipated values of 357.14 mg/g and 333.33 mg/g, respectively. The PFO rate constant (k_1) ranged from 4.15×10^{-3} to 5.53×10^{-3}, whereas the PSO rate constant (k_2) varied from 12.49×10^{-4} to 95.51×10^{-4}. These results demonstrate the PSO model's higher prediction accuracy for the adsorption kinetics of textile effluent on biochar.

The observed reduction in adsorption capacity at higher doses implies that physisorption is the primary process, whereas at lower dosages, chemisorption takes precedence. The increased adsorption capacity of KBC can be due to its bigger surface area and improved pore dispersion, as proven by BET analysis. Figure 12 depicts two separate stages: effluent diffusion onto the adsorbents' exterior surfaces (KBC and NBC), followed by intraparticle diffusion within the adsorbent surface. The curve's departure from the origin indicates that pore diffusion alone cannot account for the elimination process. KBC has higher correlation coefficients, indicating that its pore distribution and pore radius are more uniform than NBC, which is corroborated by the BET study. The increasing value of C indicates that at larger concentrations and constant adsorbent doses, the boundary layer effect or surface adsorption (physisorption) becomes more significant, whereas chemisorption takes precedence at lower adsorbent dosages. This conclusion emphasises the role of adsorption dose in determining the relative dominance of physisorption over chemisorption in wastewater treatment.

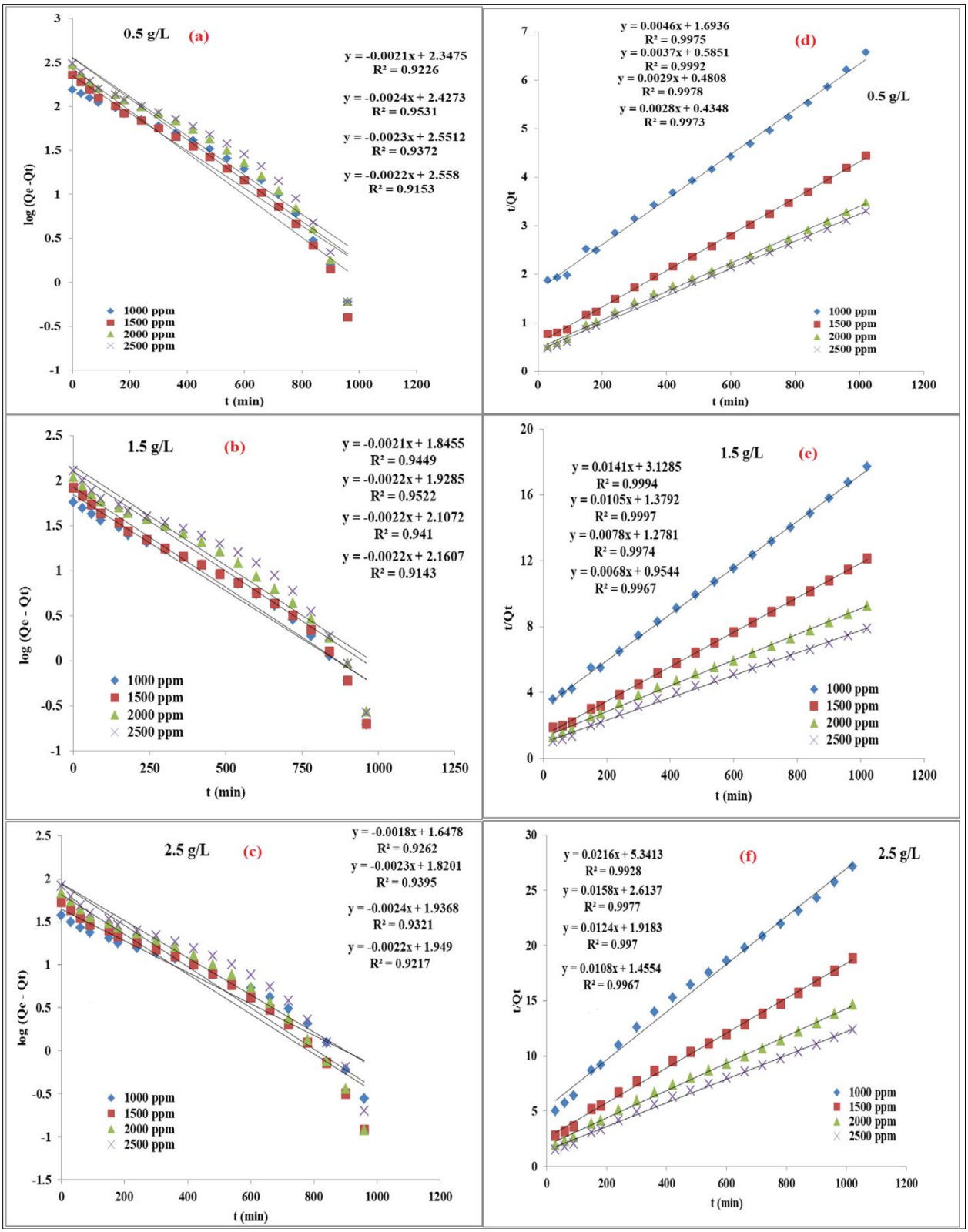

Figure 10 Adsorption Kinetic Models (a, b, c) Pseudo First order (d, e, f) Pseudo Second order for KBC

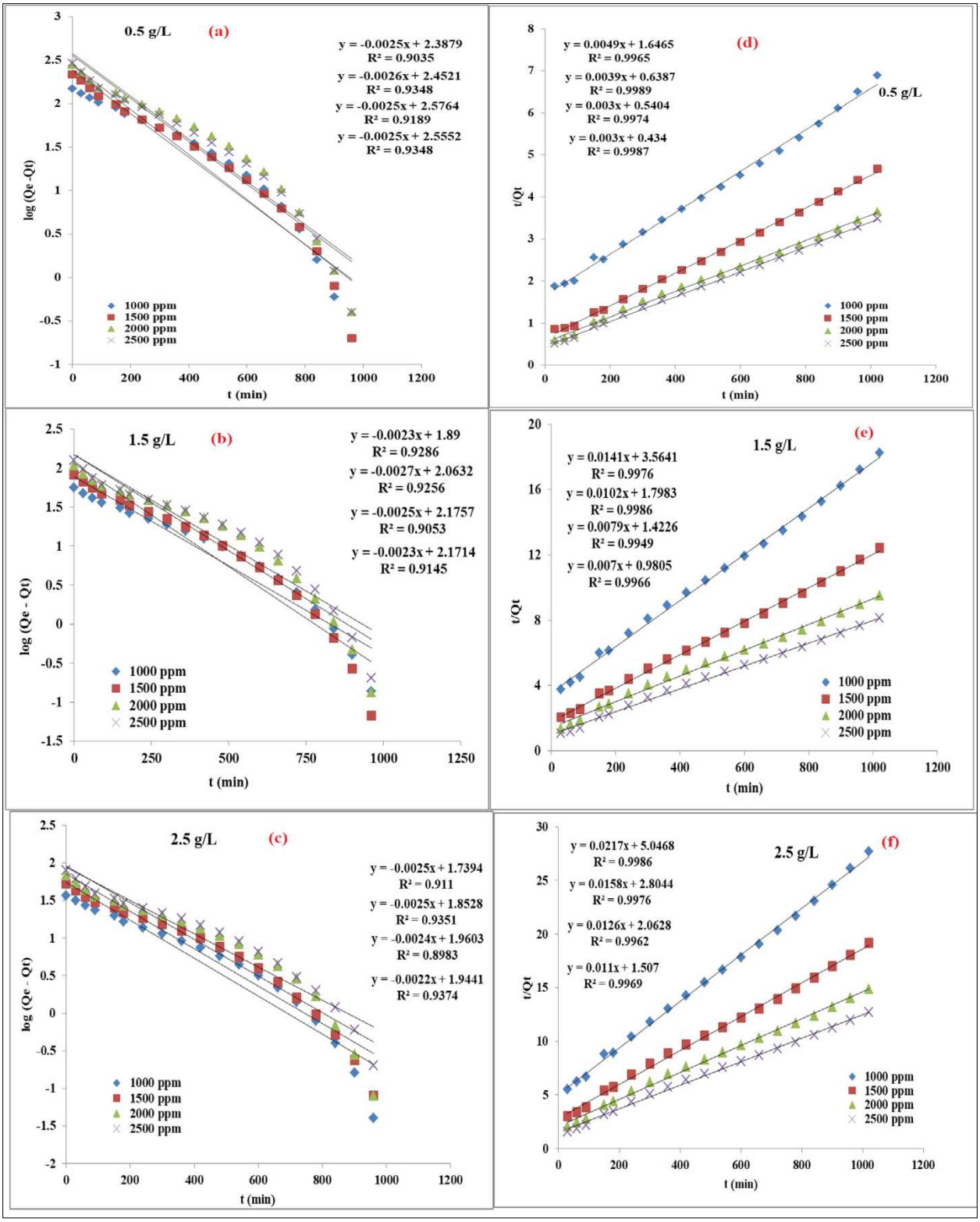
0.5 g/L
(a)
y = -0.0025x + 2.3879
R² = 0.9035
y = -0.0026x + 2.4521
R² = 0.9348
y = -0.0025x + 2.5764
R² = 0.9189
y = -0.0025x + 2.5552
R² = 0.9348
log (Qe -Qt)
t (min)
1000 ppm
1500 ppm
2000 ppm
2500 ppm
(d)
y = 0.0049x + 1.6465
R² = 0.9965
y = 0.0039x + 0.6387
R² = 0.9989
y = 0.003x + 0.5404
R² = 0.9974
y = 0.003x + 0.434
R² = 0.9987
0.5 g/L
t/Qt
t (min)
1000 ppm
1500 ppm
2000 ppm
2500 ppm
1.5 g/L
(b)
y = -0.0023x + 1.89
R² = 0.9286
y = -0.0027x + 2.0632
R² = 0.9256
y = -0.0025x + 2.1757
R² = 0.9053
y = -0.0023x + 2.1714
R² = 0.9145
log (Qe - Qt)
t (min)
1000 ppm
1500 ppm
2000 ppm
2500 ppm
(e)
1.5 g/L
y = 0.0141x + 3.5641
R² = 0.9976
y = 0.0102x + 1.7983
R² = 0.9986
y = 0.0079x + 1.4226
R² = 0.9949
y = 0.007x + 0.9805
R² = 0.9966
t/Qt
t (min)
1000 ppm
1500 ppm
2000 ppm
2500 ppm
2.5 g/L
(c)
y = -0.0025x + 1.7394
R² = 0.911
y = -0.0025x + 1.8528
R² = 0.9351
y = -0.0024x + 1.9603
R² = 0.8983
y = -0.0022x + 1.9441
R² = 0.9374
log (Qe - Qt)
t (min)
1000 ppm
1500 ppm
2000 ppm
2500 ppm
(f)
2.5 g/L
y = 0.0217x + 5.0468
R² = 0.9986
y = 0.0158x + 2.8044
R² = 0.9976
y = 0.0126x + 2.0628
R² = 0.9962
y = 0.011x + 1.507
R² = 0.9969
t/Qt
t (min)
1000 ppm
1500 ppm
2000 ppm
2500 ppm

Figure 11 Adsorption Kinetic Models (a, b, c) Pseudo First order (d, e, f) Pseudo Second order for NBC

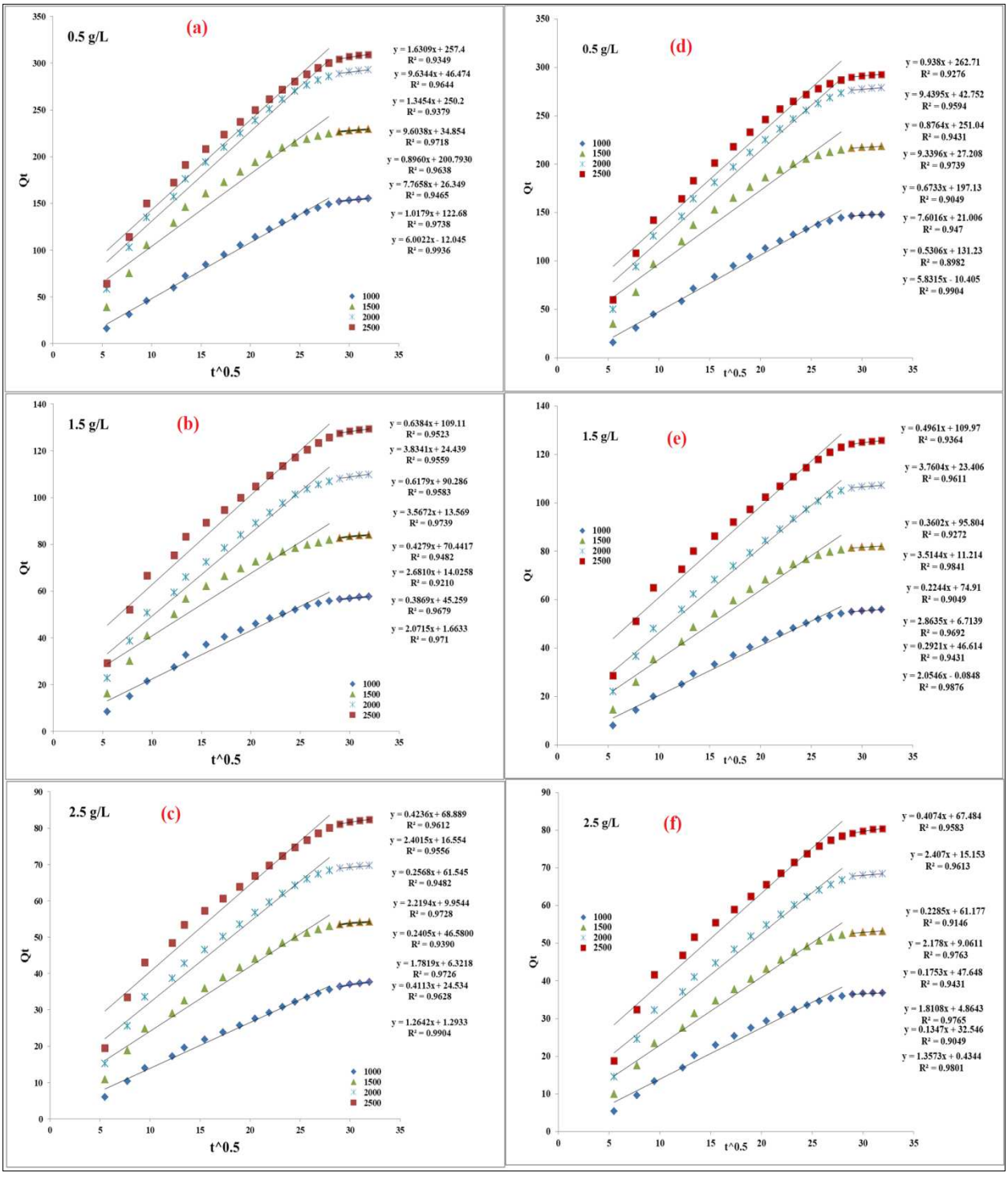

Figure 12 Intra particle diffusion model for KBC (a, b, c) and NBC (d, e, f)

3.6 Adsorption isotherm study

Understanding adsorption behaviour and selecting an appropriate isotherm model are critical for successful COD and colour removal from wastewater. These models illustrate how the adsorbate interacts with the aqueous phase and solid adsorbent over time, eventually reaching equilibrium. Various isotherm models, including Langmuir, Freundlich, Temkin, Dubinin-Radushkevich, Elovich, and Halsey, were employed to study the adsorption process on biochar. The best-fitting model was chosen based on the coefficient of determination (R^2), a measure of linear regression accuracy.

The linear form of models employed can be expressed as in equations (8-13):

$$\frac{C_e}{q_e} = \frac{1}{q_m K_L} + \frac{C_e}{q_m} \tag{8}$$

$$log q_e = \frac{1}{n} log C_e + log K_F \tag{9}$$

$$q = \frac{RT}{b} (\ln C_e + \ln K_t) \tag{10}$$

$$\ln q_e = \ln q_m - \beta \varepsilon^2 \tag{11}$$

$$\ln \frac{q_e}{C_e} = -\frac{q_e}{q_m} + \ln K_E q_m \tag{12}$$

$$\log q_e = -\frac{1}{n_H} \ln C_e + \frac{1}{n_H} \ln K_H \tag{13}$$

In this context, qe, qm, and Ce refer to the dye amount adsorbed at equilibrium, the adsorbent's maximum adsorption capacity, and the dye concentration at equilibrium, respectively. The constants KL, KF, n, KT, b, β, KE, KH, and nH correspond to the parameters of the Langmuir, Freundlich, Temkin, D-R, Elovich, and Halsey isotherms. The value of n indicates adsorption intensity, ranging from 1 to 10, which suggests favorable adsorption conditions. R denotes the Universal gas constant, and T represents temperature.

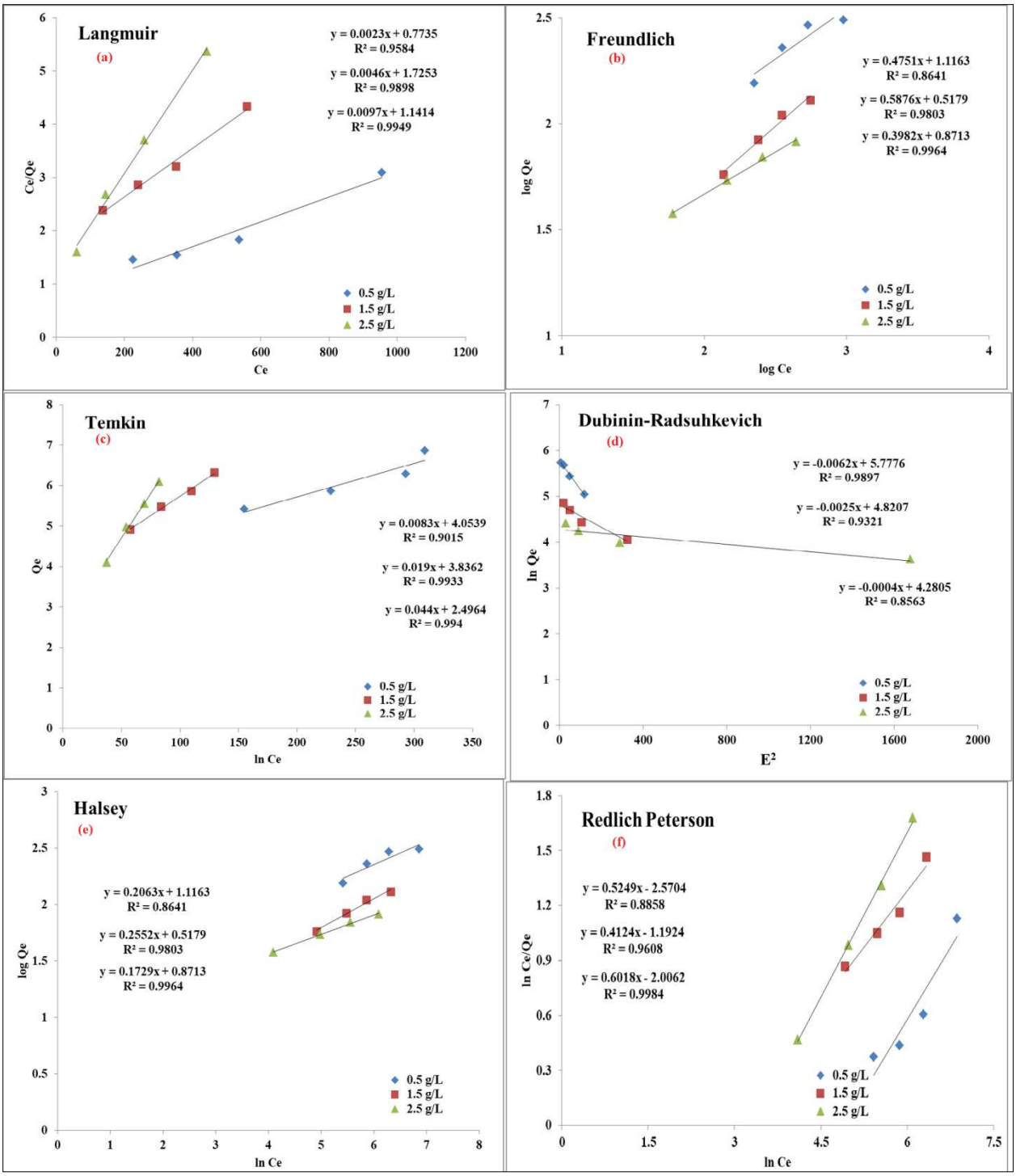

Figure 13 Adsorption isotherm models (a) Langmuir (b) Freundlich (c) Temkin (d) Dubinin-Radushkevich (e) Halsey (f) Redlich-Peterson for KBC

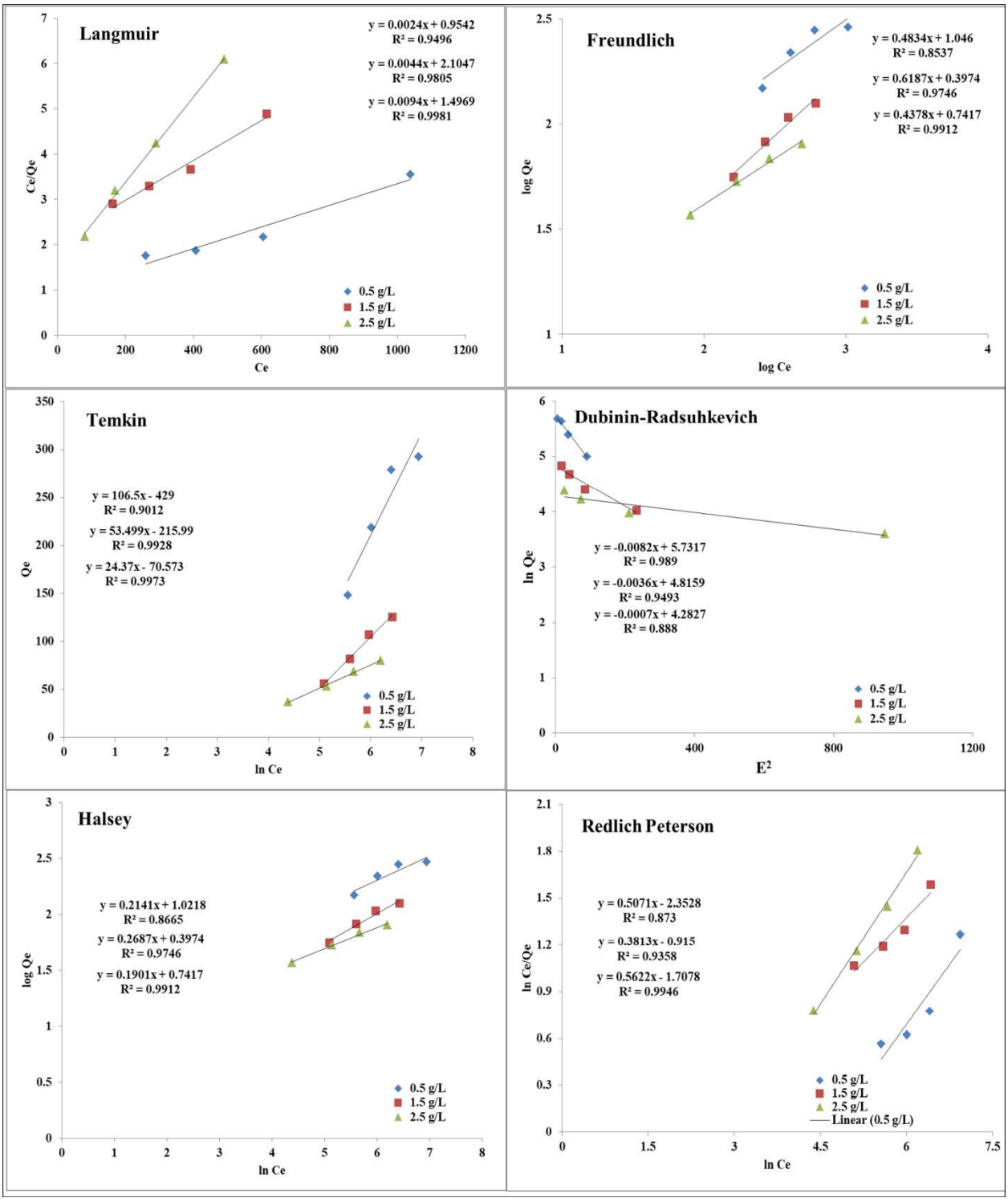

Figure 14 Adsorption isotherm models (a) Langmuir (b) Freundlich (c) Temkin (d) Dubinin-Radushkevich (e) Halsey (f) Redlich-Peterson for NBC

Figures 13 and 14, as well as Table 8, show that the Langmuir isotherm gives the greatest match for the experimental data from KBC and NBC, as evidenced by strong correlation coefficient values. The rise in KL value with increasing adsorbent doses indicates a more intense interaction between the adsorbent and adsorbate. A high R^2 value at increasing adsorbent doses suggests that surface adsorption on homogenous sites occurs more frequently at higher dosages than at lower ones. Furthermore, the Freundlich isotherm's high R^2 value indicates that multilayer adsorption helps to remove COD and colour from the solution. The rising value of n indicates that as the adsorbent dose increases, so does the adsorption intensity. Similarly, a rise in KT suggests that with a constant adsorbate concentration, the binding energy between the adsorbent and adsorbate strengthens as the adsorbent dosage increases. The adsorption capacity calculated using Langmuir suggested that the KBC is better than NBC which is supported by other isotherms used for the analysis. The high R^2 of DR at the low adsorbent dosage suggested that micro-porous adsorption of impurities is prevalent in comparison to a higher dosage of adsorbent. The mean adsorption energy value suggested that chemisorption is dominant which is supported by kinetic analysis. The order of significance for isotherms based on R^2 is found as Langmuir > Temkin > Redlich-Peterson > Freundlich = Halsey > Dubinin-Radushkevich for KBC whereas Langmuir > Temkin > Halsey > Freundlich > Dubinin-Radushkevich > Redlich-Peterson for NBC.

Table 8 Isotherm parameters and their values for KBC and NBC

Isotherm model		KBC			NBC		
		0.5	1.5	2.5	0.5	1.5	2.5
Langmuir	q_m	434.78	217.39	103.09	416.67	227.27	106.38
	$k_L\ (10^{-3})$	2.67	2.97	8.50	2.29	9.26	14.07
	R^2	0.9584	0.9898	0.9949	0.9501	0.9805	0.9981
Freundlich	n	2.10	1.70	2.51	2.07	1.62	2.28
	k_F	13.09	3.30	7.44	11.11	2.50	5.52
	R^2	0.8636	0.9803	0.9964	0.8548	0.9746	0.9912
Temkin	b	22.91	47.48	109.70	23.27	46.31	101.66
	k_T	0.0217	0.0218	0.0837	0.0178	0.0176	0.0552
	R^2	0.9012	0.9933	0.9940	0.9026	0.9928	0.9973
DR	β	0.0062	0.0025	0.0004	0.0082	0.0036	0.0007
	q_m	323.05	124.05	72.28	308.34	123.46	72.44
	R^2	0.9900	0.9321	0.8563	0.9893	0.9493	0.8880
Halsey	n_H	-4.85	-3.92	-5.78	-4.67	-3.72	-5.26
	k_H	0.0045	0.1314	0.0065	1.24	0.23	0.02
	R^2	0.8636	0.9803	0.9964	0.8677	0.9746	0.9912
Redlich Peterson	β	0.5250	0.4124	0.6018	0.5072	0.3813	0.5622
	A	13.09	3.29	7.44	10.51	2.50	5.52
	R^2	0.8855	0.9608	0.9984	0.8741	0.9358	0.9946

3.7 Response Surface Methodology

In this study, the Response Surface Methodology-Box Behnken Design (RSM-BBD) was used to evaluate how various parameters affect COD and colour removal from wastewater. The process factors adsorbent dose, pH, contact duration, ozonation rate, and type of activated charcoal were adjusted at different levels to determine their individual and combined impacts on COD and colour removal efficiency. Table 5 shows the experimental setup, which contained four numerical variables and one categorical variable, as well as the actual and coded data. To assess the impact of these factors in the removal process, a quadratic model was created using the design matrix. The empirical link between the process variables (adsorbent dose, pH, ozonation rate, contact duration, and biochar type) and the responses (percentage of COD removal and colour removal) was derived using the experimental data presented in Tables 8 and 9, as shown in equations (14-19) in both coded and actual formats.

$$COD\ Reduction\ (\%) = 84.63 - 2.01(pH) + 9.81(AD) + 6.61(OR) + 8.69(CT) - 2.41(AD \times OR) - 3.81(AD \times CT) - 12.68(pH)^2 - 3.99(AD)^2 - 1.56(OR)^2 - 1.09(BT) \quad (14)$$

$$COD\ Removal(\%) = 76.94 + 4.78(pH) + 6.26(AD) + 3.59(OR) + 5.64(CT) - 1.82(AD \times CT) + 3.26(pH \times CT) - 13.88(pH)^2 + 5.68(AD)^2 - 0.60(BT) \quad (15)$$

An empirical equation for COD reduction (%) in terms of actual factors for KOH (equation 16) and NaOH (equation 17) as given below

$$COD\ Reduction(\%) = -172.6831 + 49.6978(pH) + 31.1852(AD) + 0.3398(OR) + 2.2163(CT) - 0.5862(AD \times CT) - 0.0567(AD \times OR) - 3.1690(pH)^2 - 3.9861(AD)^2 - 0.0009(OR)^2 \quad (16)$$

$$COD\ Reduction(\%) = -174.8655 + 49.6978(pH) + 31.1852(AD) + 0.3398(OR) + 2.2163(CT) - 0.5862(AD \times CT) - 0.0567(AD \times OR) - 3.1690(pH)^2 - 3.9861(AD)^2 - 0.0009(OR)^2 \quad (17)$$

An empirical equation in terms of actual factors for KOH (equation 18) and NaOH (equation 19) as given below

$$COD\ Removal(\%) = -148.6881 + 55.2640(pH) - 13.7349(AD) + 0.0844(OR) - 1.5605(CT) + 0.2509(pH \times CT) + 0.2804(AD \times CT) - 3.4691(pH)^2 + 5.6822(AD)^2 \quad (18)$$

$$COD\ Removal(\%) = -149.8808 + 55.2640(pH) - 13.7349(AD) + 0.0844(OR) - 1.5605(CT) + 0.2509(pH \times CT) + 0.2804(AD \times CT) - 3.4691(pH)^2 + 5.6822(AD)^2 \quad (19)$$

Table 9 ANOVA Table for % COD Removal (% CODR)

Source	Sum of Squares	Contribution	Degree of Freedom	Mean Squares	F-value	p-Value Prob>F
Model	7722.85	96.11	10	772.29	116.13	< 0.0001
AD	2310.45	29.22	1	2310.45	347.42	< 0.0001
pH	97.28	1.23	1	97.28	14.63	0.0004
OR	1047.82	13.25	1	1047.82	157.56	< 0.0001
CT	1812.73	22.92	1	1812.73	272.58	< 0.0001
BT	69.06	0.87	1	69.06	10.38	0.0023
AD*OR	46.46	0.59	1	46.46	6.99	0.0111
AD*CT	116.13	1.47	1	116.13	17.46	0.0001
AD^2	213.78	2.70	1	213.78	32.15	< 0.0001
pH^2	2161.93	27.34	1	2161.93	325.08	< 0.0001
OR^2	32.74	0.41	1	32.74	4.92	0.0314
Residual	312.57	3.89	47	6.65		
Lack of Fit	312.57		39	8.01		
Pure Error	0.00		8	0.00		
Cor. Total	8035.42		57			

R^2 = 0.9611; Adj. R^2 = 0.9528; Pred. R^2 = 0.9405; Ad. Prec. = 39.54; C.V% = 3.35

Table 10 ANOVA table for % Color Removal (% COLR)

Source	Sum of Squares	Contribution	Degree of Freedom	Mean Squares	F-value	P-value Prob>F
Model	6159.58	96.96	9	684.40	169.84	< 0.0001
AD	939.25	16.21	1	939.25	233.08	< 0.0001
pH	549.32	9.45	1	549.32	136.32	< 0.0001
OR	308.67	5.33	1	308.67	76.60	< 0.0001
CT	762.19	13.15	1	762.19	189.15	< 0.0001
BT	20.63	0.36	1	20.63	5.12	0.0282
AD*CT	26.57	0.46	1	26.57	6.59	0.0134
pH*CT	85.09	1.7	1	85.09	21.11	< 0.0001
AD^2	445.70	7.69	1	445.70	110.60	< 0.0001
pH^2	2658.05	45.86	1	2658.05	659.62	< 0.0001
Residual	193.42	3.04	48	4.03		

Lack of Fit	193.42	40	4.84
Pure Error	0.00	8	0.00
Cor. Total	6353.00	57	

R^2 = 0.9696; Adj. R^2 = 0.9638; Pred. R^2 = 0.9474; Ad. Prec. = 51.39; C.V% = 2.73

Table 1 shows that the projected values from the RSM-BBD quadratic model closely match the experimental data. The ANOVA findings in Tables 9 and 10 indicate that the models are sufficient and statistically significant. The high F-values for percent COD elimination (116.13) and percent colour removal (169.84) highlight the model's statistical validity. A p-value of less than 0.0001 implies that both % COD elimination and % colour removal is highly significant. The model's accuracy was confirmed by coefficients of determination (R^2) and adjusted R^2 values of 0.9611 and 0.9528 for COD removal, and 0.9696 and 0.9638 for colour removal. Furthermore, the low coefficient of variation values for both responses (3.35% for COD and 2.79% for colour) suggest that the model is consistent and reliable as indicated by equations (x-xv). ANOVA analysis [20-21] shows that linear terms like adsorbent dosage (AD), pH, ozonation rate (OR), contact time (CT), and biochar type (BC), as well as quadratic terms like AD^2, pH^2, and OR^2, and cross-product terms like ADOR and ADCT, are statistically significant with p-values below 0.05. The most important parameters for % COD and % COL elimination was found to be adsorbent dose, pH, and contact duration.

The optimal parameters for % COD and % COL removal was statistically predicted as follows: for NBC, an adsorbent dosage of 2.5 g/L, pH 8.25, an ozonation rate of 67.56 mL/min, and a contact length of 17 hours resulted in 96.88% COD R and 98.57% COL R, with 98.57% desirability. KBC's characteristics were an adsorbent dosage of 2.5 g/L, a pH of 8.21, an ozonation rate of 79.48 mL/min, and a contact length of 17 hours, yielding 95.66% COD R and 98.23% COL R with 98% desirability. The experimental validation showed that NBC had 94.33% COD R and 93.6% COL R, whereas KBC had 93.76% COD R and 95.4% COL R.

Conclusion

This study assessed the efficacy of adsorption followed by ozonation in treating wastewater from a working textile mill to remove colour and COD. The findings imply that Canna indica may be used as an excellent adsorbent in the adsorption process to remove dyes and chemical oxygen requirement. KOH-activated biochar at a 1.5 g/L adsorbent dose resulted in 99% colour removal

and a 96.67% decrease in COD. The RSM-BBD study demonstrated that pH had a substantial impact on the adsorption process and subsequent ozonation for COD and colour removal. KOH-activated biochar (KBC) had a maximum adsorption capacity of 357.14 mg/g, exceeding non-activated biochar (NBC) with a capacity of 333.33 mg/g. KOH-treated biochar outperformed NaOH-treated biochar in terms of adsorption capacity. pH was shown to be more important than adsorbent dose, duration, and ozonation rate. Langmuir > Temkin > Redlich-Peterson > Freundlich = Halsey > Dubinin-Radushkevich is the order of importance for isotherms in KBC, but in NBC, it is Langmuir > Temkin > Halsey > Freundlich > Dubinin-Radushkevich > Redlich-Peterson.

Authors contributions:

Vishal Kumar U. Shah, Pratima Gajbhiye, Anand Mohan Yadav - Conceptualization, analysis Aparna Singh , Aditee Pandya, Md irfanul Haque Siddiqui, Choon Kit Chang, Saurav Dixit, Anand Patel – Writing original draft, Editing, methodology, Supervison

Conflict of interests:

There is no conflict of interests among authors

Data Availability:

Data used in the work is included in the paper.

References

1. Slama, HB., Chenari, BA., Pourhassan, Z., Alenezi, FN., Silini A, Cherif-Silini H, & Belbahri L (2021) *Diversity of synthetic dyes from textile industries, discharge impacts and treatment methods*. Applied Sciences, 11(14):6255. https://doi.org/10.3390/app11146255
2. Akbar, NA., & Sabri, S., Bakar, AA., & Azizan, NS., (2019) *Removal of colour using banana stem adsorbent in textile wastewater*. In Journal of Physics: Conference Series (Vol. 1349:1, 012091). IOP Publishing. DOI: - https://doi.org/10.1088/1742-6596/1349/1/012091

3. Tan, W., Wang, L., Yu, H., Zhang, H., Zhang, X., Jia, Y., & Xi, B., (2019) *Accelerated microbial reduction of azo dye by using biochar from iron-rich-biomass pyrolysis*. Materials, 12:7, 1079. https://doi.org/10.3390/ma12071079
4. Khaled, A., Nemr, AE., Sikaily, AE., & Abdelwahab, O., (2009) *Removal of Direct N Blue-106 from artificial textile dye effluent using activated carbon from orange peel: adsorption isotherm and kinetic studies*. Journal of Hazardous Materials, 165(1-3), 100-110.https://doi.org/10.1016/j.jhazmat.2008.09.122
5. Nautiyal, P., Subramanian, KA., & Dastidar, MG., (2016) *Adsorptive removal of dye using biochar derived from residual algae after in-situ transesterification: alternate use of waste of biodiesel industry*. Journal of environmental management, 182, 187-197. https://doi.org/10.1016/j.jenvman.2016.07.063
6. Tounsadi, H., Metarfi. Y., Barka, N., Taleb, M., & Rais, Z., (2020) *Removal of textile dyes by chemically treated sawdust of acacia: kinetic and equilibrium studies*. Journal of Chemistry, 2020, 1-12. https://doi.org/10.1155/2020/7234218
7. Tara, N., Siddiqui, SI., Rathi, G., Chaudhry, SA., & Asiri, AM., (2020) *Nano-engineered adsorbent for the removal of dyes from water*: A review. Current Analytical Chemistry, 16(1), 14-40. https://doi.org/10.2174/1573411015666190117124344
8. Gupta, VK., Tyagi, I., Agarwal, S., Sadegh, H., Ghoshekandi, RS., Yari, M., & Nejat, OY., (2015) *Experimental study of surfaces of hydrogel polymers HEMA, HEMA–EEMA–MA, and PVA as adsorbent for removal of azo dyes from liquid phase*. Journal of Molecular Liquids, 206, 129-136. https://doi.org/10.1016/j.molliq.2015.02.015
9. Ozdemir, O., Turan, M., Turan, AZ., Faki, A., & Engin, AB., (2009) *Feasibility analysis of color removal from textile dyeing wastewater in a fixed-bed column system by surfactant-modified zeolite* (SMZ). Journal of Hazardous Materials, 166(2-3), 647-654. https://doi.org/10.1016/j.jhazmat.2008.11.123
10. Lin, JX., Zhan, SL., Fang, MH., Qian, XQ., & Yang, H., (2008) *Adsorption of basic dye from aqueous solution onto fly ash*. Journal of Environmental Management, 87:1, 193-200. https://doi.org/10.1016/j.jenvman.2007.01.001
11. Dutta, S., Gupta, B., Srivastava, SK., & Gupta, AK., (2021) *Recent advances on the removal of dyes from wastewater using various adsorbents: A critical review*. Materials Advances, 2(14), 4497-4531. DOI: 10.1039/D1MA00354B

12. Yamjala, K., Nainar, MS., & Ramisetti, NR., (2016) *Methods for the analysis of azo dyes employed in food industry – a review*. Food chemistry, 192, 813-824. https://doi.org/10.1016/j.foodchem.2015.07.085
13. Kashefialasl, M., Khosravi, M., Marandi, R., & Seyyedi, K., (2006) *Treatment of dye solution containing colored index acid yellow 36 by electrocoagulation using iron electrodes*. International Journal of Environmental Science and Technology, 2(4), 365.
14. Xiao, H., Zhao, T., Li, CH., & Li, MY., (2017) *Eco-friendly approaches for dyeing multiple type of fabrics with cationic reactive dyes*. Journal of Cleaner Production, 165, 1499-1507. https://doi.org/10.1016/j.jclepro.2017.07.174
15. Barba, D., Beolchini, F., & Vegliò, F., (2001) *A simulation study on biosorption of heavy metals by confined biomass in UF/MF membrane reactors*. Hydrometallurgy, 59(1), 89-99. https://doi.org/10.1016/S0304-386X(00)00144-4
16. Ahluwalia, SS., & Goyal, D., (2007) *Microbial and plant derived biomass for removal of heavy metals from wastewater*. Bioresource technology, 98(12), 2243-2257. https://doi.org/10.1016/j.biortech.2005.12.006
17. Bulgariu, L., & Bulgariu, D., (2018) *Functionalized soy waste biomass-A novel environmental-friendly biosorbent for the removal of heavy metals from aqueous solution*. Journal of Cleaner Production, 197, 875-885. https://doi.org/10.1016/j.jclepro.2018.06.261
18. Oyebamiji, OO., Boeing, WJ., Holguin, FO., Ilori, O., & Amund, O., (2019) *Green microalgae cultured in textile wastewater for biomass generation and biodetoxification of heavy metals and chromogenic substances*. Bioresource Technology Reports, 7, 100247. https://doi.org/10.1016/j.biteb.2019.100247
19. Camila dos Santos, CSL., Reis, MHM., Cardoso, VL., & de Resende, MM., (2019) *Electrodialysis for removal of chromium (VI) from effluent: Analysis of concentrated solution saturation*. Journal of Environmental Chemical Engineering, 7:5,103380. https://doi.org/10.1016/j.jece.2019.103380
20. Heiderscheidt, E., Postila, H., & Leiviskä, T., (2020) *Removal of metals from wastewaters by mineral and biomass-based sorbents applied in continuous-flow continuous stirred tank reactors followed by sedimentation*. Science of the Total Environment, 700, 135079. https://doi.org/10.1016/j.scitotenv.2019.135079

21. Shukrullah, S., Azam, M., Naz, MY., Toqeer, I., & Gungor, A., (2021) *Effective removal of chromium from wastewater with Zn doped Ni ferrite nanoparticles produced using co-precipitation method*. Materials Today: Proceedings, 47, S9-S12. https://doi.org/10.1016/j.matpr.2020.04.263
22. Wang, Z., Shen, Q., Xue, J., Guan, R., Li, Q., Liu, X., Jia, H., & Wu, Y., (2020) *3D hierarchically porous NiO/NF electrode for the removal of chromium (VI) from wastewater by electrocoagulation*. Chemical Engineering Journal, 402, 126151. https://doi.org/10.1016/j.cej.2020.126151
23. Park, HG., Kim, TW., Chae, MY., & Yoo, IK., (2007) *Activated carbon-containing alginate adsorbent for the simultaneous removal of heavy metals and toxic organics*. Process Biochemistry, 42:10, 1371-1377. https://doi.org/10.1016/j.procbio.2007.06.016
24. Meena, AK., Kadirvelu, K., Mishra, GK., Rajagopal, C., & Nagar, PN., (2008) *Adsorptive removal of heavy metals from aqueous solution by treated sawdust (Acacia Arabica*). Journal of Hazardous Materials, 150:3, 604-611. https://doi.org/10.1016/j.jhazmat.2007.05.030
25. Gkika, DA., Mitropoulos, AC., & Kyzas, GZ., (2022) *Why reuse spent adsorbents? The latest challenges and limitations*. Science of the Total Environment, 822, 153612. https://doi.org/10.1016/j.scitotenv.2022.153612
26. Deng, J., Xiong, T., Xu, ., Li, M., Han, C., Gong, Y., Wang, H., & Wang, Y., (2015) *Inspired by bread leavening: one-pot synthesis of hierarchically porous carbon for supercapacitors*. Green Chemistry, 17(7), 4053-4060. https://doi.org/10.1039/C5GC00523J
27. Chen, W., Yang, H., Chen, Y., Chen, X., Fang, Y., & Chen, H., (2016) *Biomass pyrolysis for nitrogen-containing liquid chemicals and nitrogen-doped carbon materials*. Journal of analytical and applied pyrolysis, 120, 186-193.https://doi.org/10.1016/j.jaap.2016.05.004
28. Wang, J., Nie, P., Ding, B., Dong, S., Hao, X., Dou, H., & Zhang, X., (2017) *Biomass derived carbon for energy storage devices*. Journal of materials chemistry A, 5(6), 2411-2428. https://doi.org/10.1039/C6TA08742F
29. Chen, W., Gong, M., Li, K., Xia, M., Chen, Z., Xiao, H., Fang, Y., Chen, Y., Yang, H, & Chen, H., (2020) *Insight into KOH activation mechanism during biomass pyrolysis:*

Chemical reactions between O-containing groups and KOH. Applied Energy, 278, 115730. https://doi.org/10.1016/j.apenergy.2020.115730

30. Liew, RK., Azwar, E., Yek, PNY., Lim, XY., Cheng, CK., Ng, JH., Jusoh, A., Lam, WH., Ibrahim, MD., Ma, NL., & Lam, SS., (2018) *Microwave pyrolysis with KOH/NaOH mixture activation: a new approach to produce micro-mesoporous activated carbon for textile dye adsorption*. Bioresource technology, 266, 1-10. https://doi.org/10.1016/j.biortech.2018.06.051
31. Azargohar, R., & Dalai, AK., (2008) *Steam and KOH activation of biochar: Experimental and modeling studies*. Microporous and Mesoporous Materials, 110(2-3), 413-421. https://doi.org/10.1016/j.micromeso.2007.06.047
32. Veli, S., Arslan, A., Isgoren, M., Bingol, D., & Demiral, D., (2021) *Experimental design approach to COD and color removal of landfill leachate by the electrooxidation process*. Environmental Challenges, 5, 100369. https://doi.org/10.1016/j.envc.2021.100369
33. Yadav, AM., Nikkam, S., Gajbhiye, P., & Tyeb, MH., (2017) *Modeling and optimization of coal oil agglomeration using response surface methodology and artificial neural network approaches*. International Journal of Mineral Processing, 163:55-63. https://doi.org/10.1016/j.minpro.2017.04.009
34. Yadav, AM., Nikkam, S., Sundaram, A., Painkra, P., Raja, AK., & Arshad, Md., (2018) *Investigation and optimization of the recovery of coal fines using oil agglomeration process: Use of waste oils from different sectors*. Journal of Dispersion Science and Technology 39:5, 754-764. https://doi.org/10.1080/01932691.2017.1414610
35. Yadav, AM., Chaurasia, RC., Suresh, N., & Gajbhiye, P., (2018) *Application of artificial neural networks and response surface methodology approaches for the prediction of oil agglomeration process*. Fuel, 220:826-836. https://doi.org/10.1016/j.fuel.2018.02.040
36. Li, B., Huang, L., Lv, X., & Ren, Y., (2021) *Study on temperature variation and pore structure evolution within coal under the effect of liquid nitrogen mass transfer*. ACS Omega, 6:30, 19685-19694. https://doi.org/10.1021/acsomega.1c02331
37. Rangabhashiyam, S., & Balasubramanian, P., (2019) *The potential of lignocellulosic biomass precursors for biochar production: performance, mechanism and wastewater application-a review*. Industrial Crops and Products, 128, 405-423.

DOI :10.1016/j.indcrop.2018.11.041

38. Ahuja, R., Kalia, A., Sikka, R., & Chaitra, P., (2022) *Nano Modifications of Biochar to Enhance Heavy Metal Adsorption from Wastewaters: A Review*. ACS Omega, 7:50, 45825-45836. https://doi.org/10.1021/acsomega.2c05117
39. Ghanim, B., O'Dwyer, TF., Leahy, JJ., Willquist, K., Courtney, R., Pembroke, JT., & Murnane, JG., (2020) *Application of KOH modified seaweed hydrochar as a biosorbent of Vanadium from aqueous solution: Characterisations, mechanisms and regeneration capacity*. Journal of Environmental Chemical Engineering, 8:5, 104176. https://doi.org/10.1016/j.jece.2020.104176
40. Wang, S., Nam, H., & Nam, H., (2020) *Preparation of activated carbon from peanut shell with KOH activation and its application for H_2S adsorption in confined space*. Journal of Environmental Chemical Engineering, 8:2, 103683. https://doi.org/10.1016/j.jece.2020.103683
41. Surip, SN., Abdulhameed, AS., Garba, ZN., Syed-Hassan, SSA., Ismail, K., & Jawad, AH., (2020) *H_2SO_4-treated Malaysian low rank coal for methylene blue dye decolourization and cod reduction: optimization of adsorption and mechanism study*. Surfaces and Interfaces, 21, 100641. https://doi.org/10.1016/j.surfin.2020.100641
42. Devi, R., Singh, V., & Kumar, A., (2008) *COD and BOD reduction from coffee processing wastewater using Avacado peel carbon*. Bioresource technology, 99:6, 1853-1860. https://doi.org/10.1016/j.biortech.2007.03.039
43. Muthukumar, M., Sargunamani, D., Selvakumar, N., & Rao, JV., (2004) *Optimisation of ozone treatment for colour and COD removal of acid dye effluent using central composite design experiment*. Dyes and Pigments, 63:2, 127-134.https://doi.org/10.1016/j.dyepig.2004.02.003
44. Perkins, WS., Law, SE., Smith, MC., Winger, PV., & Lasier, PJ., (2001) *Biological Treatability and Environmental Impact of Ozonation of Spent Reactive Dyebaths*. AATCC Review, 1(2).
45. Körbahti, Bahadır K., and Abdurrahman Tanyolaç. *"Electrochemical treatment of simulated textile wastewater with industrial components and Levafix Blue CA reactive dye: Optimization through response surface methodology."* Journal of hazardous Materials 151.2-3 (2008): 422-431. https://doi.org/10.1016/j.jhazmat.2007.06.010

46. Asgari, Ghorban., et al. *"Sonophotocatalytic treatment of AB113 dye and real textile wastewater using ZnO/persulfate: Modeling by response surface methodology and artificial neural network."* Environmental research 184 (2020): 109367. https://doi.org/10.1016/j.envres.2020.109367
47. Sharma, S., S. Kapoor., & R A, Christian., *"Effect of Fenton process on treatment of simulated textile wastewater: optimization using response surface methodology."* International Journal of Environmental Science and Technology 14 (2017): 1665-1678. https://doi.org/10.1007/s13762-017-1253-y
48. Bashir, Mohammed JK., et al. *"Wastewater treatment processes optimization using response surface methodology (RSM) compared with conventional methods: review and comparative study."* Middle-East J. Sci. Res 23.2 (2015): 244-252. https://doi.org/10.5829/idosi.mejsr.2015.23.02.52
49. Vyavahare, Govind D., et al. *"Response surface methodology optimization for sorption of malachite green dye on sugarcane bagasse biochar and evaluating the residual dye for phyto and cytogenotoxicity."* Chemosphere 194 (2018): 306-315. https://doi.org/10.1016/j.chemosphere.2017.11.180
50. Roy, Hridoy., et al. *"Synthesis, characterizations, and RSM analysis of Citrus macroptera peel derived biochar for textile dye treatment."* South African Journal of Chemical Engineering 41 (2022): 129-139. https://doi.org/10.1016/j.sajce.2022.05.008
51. Perveen, Shazia., et al. *"Biochar-mediated zirconium ferrite nanocomposites for tartrazine dye removal from textile wastewater."* Nanomaterials 12.16 (2022): 2828. https://doi.org/10.3390/nano12162828
52. Jagaba, Ahmad., & Hussaini., et al. *"Biochar-based geopolymer nanocomposite for COD and phenol removal from agro-industrial biorefinery wastewater: kinetic modelling, microbial community, and optimization by response surface methodology."* Chemosphere 339 (2023): 139620. https://doi.org/10.1016/j.chemosphere.2023.139620
53. Fseha., Yohanna, Haile., Jamal, Shaheen., & Banu, Sizirici., *"Phenol contaminated municipal wastewater treatment using date palm frond biochar: Optimization using response surface methodology."* Emerging Contaminants 9.1 (2023): 100202. https://doi.org/10.1016/j.emcon.2022.100202

54. Husien, Sh., et al. *"Review of activated carbon adsorbent material for textile dyes removal: Preparation, and modelling."* Current Research in Green and Sustainable Chemistry (2022): 100325. https://doi.org/10.1016/j.crgsc.2022.100325
55. Laxmi, Deepak Bhatlu., M., et al. *"Preparation of Breadfruit Leaf Biochar for the Application of Congo Red Dye Removal from Aqueous Solution and Optimization of Factors by RSM-BBD."* Adsorption Science & Technology 2023 (2023). https://doi.org/10.1155/2023/7369027
56. Saravanan, Praveen., et al. *"Evaluation of the adsorptive removal of cationic dyes by greening biochar derived from agricultural bio-waste of rice husk."* Biomass Conversion and Biorefinery (2021): 1-14. https://doi.org/10.1007/s13399-021-01415-y
57. Kapoor, Riti Thapar., & Selvaraju ,Sivamani., *"Adsorptive Potential of Orange Peel Biochar for Removal of Basic Red 46 Dye and Phytotoxicity Analysis."* Chemical Engineering & Technology 46.4 (2023): 756-765. https://doi.org/10.1002/ceat.202200436